

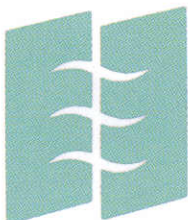
FIBRE DIFFRACTION REVIEW

THE CCP13 NEWSLETTER
Software Development for Fibre Diffraction

Issue 5

December 1996

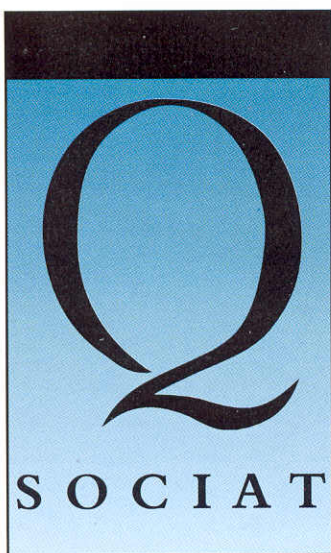
Specialist users require specialist data storage solutions



LEGATO™

StorageWorks

Q Associates specialises in the supply of data storage solutions and computer systems to research and academic users in the UNIX environment. With extensive knowledge of Digital, Sun SPARC, SGI, IBM RS/6000 and Hewlett-Packard platforms, the company provides a full range of high capacity disk, tape and optical solutions for stand-alone or networked configurations.



**For more information:
Tel: 01635 248181
Fax: 01635 247616
Email: academic@qassoc.co.uk**

**Q Associates Limited
Langley Business Court, Beedon,
Newbury, Berkshire RG20 8RY**

A S S O C I A T E S

Contents

Contents, Cover Caption & Production	1
The CCP13 Committee Members	2
Chairman's Message	3
Report on the 1996 IUCr, Seattle, J.Harford	4
Report on SAS96, Campinas, Brazil, P.Fairclough	5
Report on the 5th CCP13/NCD Workshop, 1996, G.Mant	7
Report on the Synchrotron Radiation Summer School, 1996 Italy, J.Squire	9
CCP13 Program Updates, R.Denny	11
Summary of Available CCP13/NCD Software	13

Contributed Articles

Collagen Fibril Orientations in Tissues and their Relationship to Mechanical Properties, D.W.L.Hukins	14
Diffraction by Disordered Fibres, R.P.Millane and W.J.Stroud	16
Advantages of Absolute Calibration in Small-Angle X-ray and Neutron Scattering Studies of Polymers and Colloids, G.D.Wignall	21
Fibre Diffraction Spot Profiles and the Lorentz Correction, R.Denny	24
3-D Reconstruction from Fibre X-ray Diffraction Patterns: Myosin-Decorated Actin Filaments, J.J.Harfard, R.C.Denny, E.Morris, R.Mendelson and J.M.Squire	27

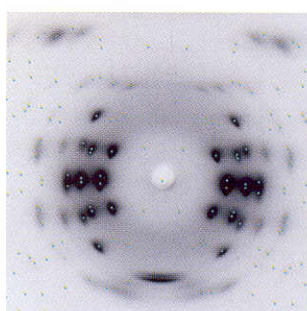
5th Annual Workshop Prize - Winning Abstracts

The "RAPID" High Rate Area X-ray Detector System, R.A.Lewis, C.Hall, B.Parker, A.Jones, W.Helsby, J.Sheldon, P.Clifford, M.Hillen and N.Fore	30
Neutron Diffraction Study of B-DNA Hydration , L.H.Pope, M.W.Shotton, V.T.Forsyth, P.Langan, H.Grimm, A.Rupprecht, R.Denny and W.Fuller	34
Chain Conformations in Polyurethanes : A SAXS & SANS Study, A.J. Ryan, S. Naylor, N.J.Terrill and S.King	38

1996 CCP13/NCD Annual Meeting Abstracts	40
CCP13 Travelling Fellowships	59
CCP13 Visiting Scientist Fellowship Programme.....	59

Forthcoming Meetings

The 6th Annual CCP13/NCD Workshop, May 7-9, 1997 Daresbury Laboratory.....	60
Coiled-Coils, Collagen & Co-Proteins II, September 7-13, 1997, Alpbach, Austria	60



Front Cover Image

An X-ray diffraction pattern of PET (polyethylene terephthalate) recorded on SRS station 7.2 at the CCLRC Daresbury Laboratory (courtesy of Dr. A. Mahendrasingam, Keele University). The unit cell parameters and the orientation of the unit cell with respect to the fibre axis have been refined using the CCP13 program, LSQINT. The Bragg sampling positions are displayed on the pattern using the new graphical user interface, XFIR.

Newsletter Production

Editor: Prof. J.Squire, Biophysics Section, Blackett Laboratory, Imperial College, London SW7 2BZ
Production: Dr. G.Mant, Dr. R.Denny and Mr S.Eyres, CCLRC Daresbury Laboratory, Warrington WA4 4AD
Printer: Eaton Press, Wallasey, Merseyside, L44 7JB

The CCP13 Committee Members (1996)

Chairman Prof. John Squire (to 1999)
Biophysics Section, Blackett Laboratory, Imperial College, London SW7 2BZ
Phone 0171 594 7691 **Fax** 0171 589 0191 **Email** j.squire@ic.ac.uk

Secretary Dr Geoff Mant (to 1999)
CCLRC Daresbury Laboratory, Keckwick Lane, Daresbury, Warrington WA4 4AD
Phone 01925 603169 **Email** g.r.mant@dl.ac.uk

Research Assistant (Ex Officio) Dr Richard Denny
CCLRC Daresbury Laboratory, Keckwick Lane, Daresbury, Warrington WA4 4AD
Phone 01925 603626 **Email** r.denny@dl.ac.uk

Members

Dr Mike Ferenczi (to 1998)
National Institute for Medical Research, Ridgeway, Mill Hill, London NW7 1AA
Phone 0181 959 3666 **Email** m.ferenc@nimr.mrc.ac.uk

Dr Trevor Forsyth (to 1998)
Keele University, Physics Department, Keele, Staffs, ST5 5BG
Phone 01782 613847 **Email** pha23@cc.keele.ac.uk

Dr Manolis Pantos (to 1999)
CCLRC Daresbury Laboratory, Keckwick Lane, Daresbury, Warrington WA4 4AD
Phone 01925 603275 **Fax** 01925 603275 **Email** e.pantos@dl.ac.uk

Dr Tony Ryan (to 1997)
Manchester Materials Science Centre, UMIST, Grosvenor Street, Manchester, M1 7HS
Phone 0161 200 3614 **Email** tony.ryan@umist.ac.uk

Dr Tim Wess (to 1999)
The University of Stirling, Department of Biological and Molecular Sciences, Stirling, FK9 4LA
Phone 01786 467775 **Fax** 01786 464994 **Email** tjw3@stir.ac.uk

Members (Ex Officio)

Dr Greg Diakun
CCLRC Daresbury Laboratory, Keckwick Lane, Daresbury, Warrington WA4 4AD
Phone 01925 603343 **Email** g.diakun@dl.ac.uk

Dr Rob Lewis
CCLRC Daresbury Laboratory, Keckwick Lane, Daresbury, Warrington WA4 4AD
Phone 01925 603544 **Email** r.a.lewis@dl.ac.uk

Chairman's Message

CCP13 NEWS

The CCP13 Newsletter continues to go from strength to strength and this year, by popular demand, has been given a meatier title the 'Fibre Diffraction Review'. Following on from the successful improvement in presentation of the last (1995) issue, this edition, the fifth Newsletter, builds on this success and includes discussion of some of the recent topics taxing fibre diffractionists at the present time. It also includes abstracts from the 1996 CCP13/NCD Workshop at the Daresbury Laboratory which has become a regular feature. Additional copies of the Fibre Diffraction Review have been printed so that it will go not only to people on the CCP13 mailing list, but also to places and people regarded as influential and potentially interested or supportive. In addition, the Fibre Diffraction Review is being incorporated as part of the CCP13 World Wide Web pages (as with the previous Newsletters: details elsewhere). Articles in the current edition of the Fibre Diffraction Review illustrate some of the progress made in developing CCP13 fibre diffraction software in the past year, some ideas about the direction that CCP13 should take in the future, and application of the existing suite to a range of interesting biological and materials science problems.

As detailed in the report by G.Mant, the 1996 Annual Workshop at Daresbury was, once again, a joint meeting, with an international flavour, of CCP13 and the UK Non-Crystalline Diffraction community, reflecting the considerable overlap of interests of the two groups. The meeting was very well attended and emphasises the importance of the topic. The success of the format means that the 1997 meeting will be structured in a related way, although this time, as an experiment, being scheduled over two days rather than three. Remember not only that your poster could win a large cash prize (1st Prize - £100; 2nd Prize - £50), but also that abstracts will be included in this Annual 'Fibre Diffraction Review' (also on the WWW) - your work will be available to a worldwide audience. As usual, there will be bursaries available for students and young scientists to attend the 1997 Workshop. Details of all these are given at the end of the Newsletter.

CCP stands for Collaborative Computational Project. CCP13 is funded in the UK mainly by the Biotechnology and Biological Sciences Research

Council (BBSRC). An additional grant comes from EPSRC to help fund meetings and travel for the 'synthetic polymer' side of CCP13. CCP13 is one of 12 current CCPs run mainly by BBSRC/EPSRC. Our current CCP runs to the end of September, 1998 with BBSRC support. A CCP Steering Committee has been formed to coordinate activities of all the CCPs. The Chairman of the Committee is Prof. Dominic Tildsley (Imperial College) and the Secretary is Dr. Paul Durham (Daresbury). This Steering Committee has met twice so far and is gradually formulating the role it should play in future CCP activities.

The current BBSRC grant to CCP13 allows the continued employment of Richard Denny as the CCP13 RA and it provides funds towards Workshops, Newsletter Production and International Interactions. The funding by BBSRC and EPSRC also allows CCP13 to carry out 'good works'. At the last CCP13 Workshop it was agreed that these would be to fund a small number of 'CCP13 Travelling Fellowships' and a 'CCP13 Visiting Scientist Fellowship Program'. This year we awarded our 'CCP13 Visiting Scientist Fellowship' to Prof. Rick Millane, from the Whistler Center for Carbohydrate Research at Purdue University. Prof. Millane not only participated in the 1996 CCP13/NCD Workshop, but also visited various laboratories around the UK and gave lectures. His report is included elsewhere in this edition.

The two CCP13 Travelling Fellowships were awarded to Dr. Jeff Harford (Imperial College) and Dr. Patrick Fairclough (UMIST). Reports on their visits are also reported here. Application details for Travelling fellowships to be awarded during 1997 are given later in this issue.

Your Contribution

Interested groups or individuals are invited to contact any of the officers of CCP13 to obtain information about CCP13 Workshops, software developments, software standards and so on. Offers of home-written software that could be incorporated into the new CCP13 suite of programs would be much appreciated and will, of course, permanently carry the authors' attribution. Make sure that you are on the CCP13 mailing list and you will be kept informed.

Editorial Policy

Articles for inclusion in the Fibre Diffraction Review are welcome by the Editor at any time, but preferably items for the December 1997 issue should arrive before the end of November 1997. It is hoped that the Fibre Diffraction Review will become an Annual 'essential' for Fibre Diffractionists. This is the place to advertise your fibre diffraction or NCD meetings, to report on new software or 'hot' results obtained using the CCP13 or other fibre pattern processing suites and to provide reports of meetings of interest, preferably together with one or two photographs. All technical articles will be scrutinised both for scientific content and presentational style by the Editor (or his nominee) together with at least one other member of the CCP13 Steering Panel. In this way we hope to maintain high standards. Remember that the Newsletter not only goes to other Fibre Diffractionists, but also to various members of the Research Council Secretariats and to other funding agencies.

International Cooperation

Although these CCPs are UK funded projects, there is a very strong interest in making them international through cooperation with interested scientists in other countries. A natural link for CCP13, for example, exists with the Special Interest Group (SIG) in Fibre Diffraction of the American Crystallographic Association and possibly with some

American synchrotron users (CHESS). Others exist with the ESRF at Grenoble and with the Photon Factory in Japan.

Retirements and New Elections

At the 1996 Annual Meeting, John Squire was re-elected as CCP13 Chairman, Geoff Mant was re-elected as Secretary and Manolis Pantos was re-elected as a Committee member. Unfortunately, Dr. Rob Rule tendered his resignation from the Committee in November 1996. Rob's job has moved and he now has new commitments that make it difficult for him to continue. However, he has made a major contribution to our activities for a number of years and I am happy to express, on behalf of CCP13, our considerable appreciation of his role in helping to get CCP13 off the ground and into the healthy position that it now enjoys. The CCP13 Committee are now seeking a replacement for him. The term of office of Tony Ryan finishes at the May meeting this year; other existing Committee members all continue at least until 1998. There are therefore two positions to be filled at the CCP13 Annual General Meeting in May. Tony Ryan is prepared to stand again for election to the Committee. Other nominations for election to the Committee can be sent to the CCP13 Secretary, Dr. Geoff Mant, before the May 1997 meeting.

John Squire

IF YOU ARE A FIBRE DIFFRACTIONIST STUDYING SYNTHETIC OR BIOLOGICAL POLYMERS. THIS CCP IS FOR YOU. PLEASE HELP TO MAKE IT WORK!

1996 IUCr, Seattle

The main focus of this CCP13 sponsored visit over 10 days (August 12-22, 1996) to the USA was the attendance and presentation of an invited paper at the XVII IUCr (International Union of Crystallography) meeting in Seattle, Washington. This esteemed crystallography conference which boasted the participation of no less than eight Nobel Prize winners took place in the magnificent Washington Convention Centre over a period of nine days, the last four of which were attended. Arriving on the "rest day" I dutifully relinquished the Panoramic

Tour of Seattle to give a seminar at the Centre of Bioengineering (University of Washington) where I was most warmly hosted by Gerry Pollack. The fibre diffraction session comprised three sub-sessions including 27 papers covering synthetic polymers (chaired by Kenn Gardner), methods of structure determination (chaired by John Blackwell) and fibre diffraction of biological polymers (chaired by Rick Millane). Reports and abstracts from these sessions are all available on the IUCr WWW page (<http://www.hwi.buffalo.edu/aca/>).

In the final session on biological structures K.Namba discussed the complimentary use of X-ray fibre diffraction and electron cryomicroscopy to deduce the domain structure of the flagellin subunit in the flagellar filament; this revealed an overall folding of flagellin and direct interaction of the termini in the very inner core of the filament. M.M.Tirion discussed the use of two different methods in the refinement of the F-actin structure against 7Å X-ray fibre diffraction data. Both methods showed similar trends in the structural changes of G-actin to F-actin, including the closure of the nucleotide pocket between the large and small domains. M.Ivanova had a busier afternoon than most, presenting two talks; firstly on X-ray and neutron diffraction studies of filamentous bacteriophage M13 and Pf1 and chemically and genetically constructed variants of these particles, a topic which was widely covered with an additional contribution from G.Stubbs on his recent studies of site-directed mutagenesis of tobacco mosaic and other filamentous viruses, and secondly on a method of background estimation of these data. This uses the observation that the spatial frequencies making up the background are much lower than those that constitute the data. Iterative low pass filtering to separate the layer line data from the background and integration of this process into angular deconvolution allowed accurate estimates from patterns that could not be successfully processed by previous methods. K.Okuyama described the structural analysis of hydrated chitosan derived by deacetylation of chitin tendon showing that the transition from the hydrous to the anhydrous form requires cleavage of the NH-O6 hydrogen bond between antiparallel molecular chains and the formation of the new NH-O6 bond between parallel polymer chains. L.C.Yu showed that detailed analysis of the inner region of the first layer line in X-ray patterns from fibre bundles of skinned rabbit psoas suggests that the layer line is a mixture of overlapping thick and thin filament based layer lines and their relative contribution varies with ionic strength, correlating with the fraction of weakly bound cross-bridges. The diffuse scattering is little effected by these changes supporting the idea that the weakly attached cross-bridges assume nonstereospecific conformations. There were many other papers of particular interest on muscle and membrane protein structure and the techniques used in their crystallisation and determination. In the session on *Muscle & Motor Proteins*, C. Smith

presented the recently published structure of a fragment of myosin cross bridge crystallised with ADP vanadate as an analog of the transition state complex; this being the expected form of the cross bridge at the beginning of the power stroke. Possible conformational changes following the release of ADP during the power stroke are suggested by the high resolution cryo-electron microscopy of actin decorated with myosin cross bridges. R.Milligan showed that on addition of ADP to this preparation the distal lever arm of the cross bridge rotates through 35°.

A final very full day in Seattle at the loftiest heights of the Olympic Peninsula was followed by the presentation of a paper at the Whistler Centre for Carbohydrate Research at Purdue University (West Lafayette) where I was very kindly hosted by Rick Millane. Grant Bunker (director of BioCAT, Biophysics Collaborative Access Team) very kindly hosted a visit to the Advanced Photon Source (APS) at the Argonne National Laboratory. The BioCAT beamline, under construction at the time of this visit, will provide X-ray diffraction/scattering and X-ray absorption spectroscopy for studying biological structures and dynamics at the molecular level. Its main focus is non-crystalline systems, with an emphasis on time-resolved experiments and studies of small ordered domains (down to 50-100µm). The beamline will deliver 2.4×10^{12} ph/s/mm² without focusing of the incident beam and 5×10^{14} with the beam focused at the specimen position with a spot size <50µm (FWHM vertical) by <200µm (FWHM horizontal). The director, Grant Bunker, has assembled a very talented team including Tom Irving, Edgar Black who was in charge of engineering and installing most of the magnets in the ring and Gerd Rosenbaum who built one of the first synchrotron X-ray beamlines about 25 years ago at DESY in Hamburg for fibre diffraction studies of muscle. The remaining two days were spent on an excursion through Toronto and finally a seminar presentation at the Materials Science and Engineering Dept. of Lehigh University in Bethlehem (Pennsylvania). The next IUCr conference in 1999 will be held in Glasgow organised by Chris Gilmore.

Jeffrey Harford

SAS-96, Campinas, Brazil

In July of this year the biannual conference on Small Angle Scattering (SAS-96) was held at the university of Campinas near San Paulo Brazil. The area around San Paulo is regarded as the economic heart of Brazil with the majority of the countries wealth being created within the province. The University of Campinas (UniCamp) that is held in high regard for its achievements in the scientific arena together with the newly completed Brazilian National Synchrotron Light laboratory (NLS), located close to the campus, will provide an excellent facility for experimentalists throughout South America. This ambitious project will allow South American countries and Brazil in particular access to high quality scientific research previously only available outside the continent. The synchrotron, while not directly feeding the hungry in Brazil, will allow the Brazilian scientific community to spend its money at home, thus keeping the scientific elite within its boundaries and preventing the best scientists from leaving. It will also help the country to grow and develop with less dependence on the outside world. This in turn will aid in the feeding of the hungry and socially disadvantaged within the country. While at the conference not all the participants felt that the development of such a resource would be their first priority, many felt that the politicians in their own countries would lack the courage to accept the responsibility such a move would imply within the remit of their office. It is a brave move and, as in most cases, only time will provide the answer.

The conference was scheduled to take place in the newly completed conference hall at the university of Campinas. Unfortunately tropical storms destroyed the roof of the conference hall and we were hastily relocated to the headquarters of Brazilian Telecom, TeleBras. The conference was an opportunity to meet many of the names associated with Small angle scattering, Otto Glatter, as Liz may recall, being one of the "famous" ones. The conference had sessions devoted to all areas of Small Angle Scattering including polymers and biomaterials. With topics including structure and ordering phenomena, micellization, thin films and aggregates. Due to unfortunate circumstances I was provided with an opportunity to present a talk on our recent work on block copolymers undertaken on station 8.2 at Daresbury during the polymer session chaired by Claudine Williams. The talk was well received by those who were able to wade through the rough

northern dialect, with many contacts being formed immediately afterwards. Considerable time was devoted to the application of small angle scattering in polymeric materials. Otto Glatter's talk entitled "Amphiphilic aggregates, micelles, vesicles and microemulsions" detailing the SAXS study on ABA triblocks in aqueous solution was useful for our future studies on the EBE triblock in water system. John Penfold's talk detailing the effects of shear on concentrated micellar phases, was instructive as we have recently embarked on a study of the effects of shear on block copolymers and gels phases using rheology and SAXS techniques. Work at Daresbury was well represented both at the poster session and in the presentations. The talks by Ian Hamley, Tony Ryan (2), Wim Bras and myself and posters by Liz Towns-Andrews, Greg Diakun, Richard Denny, Ian Hamley, Tony Ryan, the detector group and myself where well received.

The tour of the synchrotron proved informative and a stimulus to discussion for the poster session that was held later on site. During the tour of the Synchrotron outside Campinas we had time to see the details of the ring and injector system, the control room and integrated software system for the control of the Synchrotron. The Small-Angle Facility was impressive, especially the ability to swing the whole beamline about the axis of the mono to facilitate the use of a variable wavelength. Prof. Iris Tossriani from Physics at UniCamp is responsible for the Small Angle Beamline and we are currently involved in a collaboration established at the conference. The use of CCD detectors and their own gas multiwire detectors, provide a foundation for the growth of experience-based in-house knowledge. This is an underpinning principle of the Synchrotron development, with all systems being designed and built in Brazil allowing an accumulation of experience coupled with the ability to perform repairs quickly without expensive overseas contractors.

The evenings were spent, as they are at most conferences, are deep in conversation on the topics of the day with little time for socialising other than at meal times. Thanks must go to our host, Prof. Aldo Craievich, who was always available and most helpful in providing support for many of the participants. He organised several outings including one to a "chasgaria" or barbecue restaurant, where

the delights of a “caiperinia” were unleashed on an unsuspecting public; well most of us were unsuspecting, except Marcia Sing, who seemed well versed in the art. The conference was a good chance to meet people from around the world involved with Small Angle Scattering, to exchange knowledge on

techniques and methods of research and to establish ongoing collaborations, some of which are now starting to produce papers on triblock copolymer systems.

Patrick Fairclough

5th Annual CCP13/NCD Workshop

The fifth annual workshop for the collaborative computational project for fibre diffraction (CCP13) and non-crystalline diffraction (NCD) was held at Daresbury on the 7th-9th of May, 1996 and attracted 72 participants. Once again the workshop covered a number of topics, including synthetic polymers, hardware sources and detectors, software developments and biological systems. The talks were complemented with a poster session and commercial exhibition sponsored by Q-Associates and Siemens.

After the Chairman's introduction, George Wignall (Oakridge), the first keynote speaker, opened the polymer session by describing the advantages of absolute calibration standards utilizing examples from supercritical polymerisation and surfactant micelles. The session continued with Nick Terrill (UMIST) describing his latest work on the various structural intermediates during polymer extrusion, as studied by on-line SAXS/WAXS. Patrick Fairclough (UMIST) then discussed the complex melt phases in the PBO-PEO diblock copolymer order diagram determined by SAXS/WAXS/DSC studies and Ian Hamley (Leeds) concluded the session with a presentation on semi-dilute diblock copolymers.

As a prelude to the poster session, individual short presentations were made by Quanning Li, Günter Grossmann, Wayne Oatway and Andy Hammersley. The first day was concluded by dinner, poster viewing and judging, the commercial exhibition and a wine reception.

The second day began with Goran Ungar (Sheffield) describing his work on self-assembly in novel thermotropic systems. John Pople (Reading) discussed the use of a CCD detector as an X-ray imaging system developed for in-situ time resolved studies on polymer deformation. Mike Butler (Cambridge) outlined a series of polymer systems studied by simultaneous 2-D SAXS/WAXS, including PE, PMMA, and HDPE. Darren Hughes (Keele) also presented 2-D SAXS/WAXS results, of

spherulites, obtained at the ESRF using a Photonic Science CCD detector and a Synoptic framegrabber. Rob Lewis (Daresbury) demonstrated his latest method for correcting gas detector data for spatial resolution and wire modulation. He then showed the preliminary results obtained from the new “RAPID” detector system. The morning session was then concluded by Mark Shotton (Keele).

After lunch, Ian Munro (Daresbury) gave a brief history of the SRS, and then outlined details of proposed upgrades and new stations, science highlights and future developments. John Squire (Imperial College) then elaborated on a proposal to upgrade station 2.2 at the SRS as a new fibre diffraction facility. He concluded by showing potential areas of research. Stephen King (Rutherford) described shear flow experiments with Pluronic P85 water soluble macro surfactant on the LOQ beamline at the ISIS facility.

After coffee, the poster prizes were awarded by J.Squire. The judges (D.Hukins and G.Wignall) decided to award prizes in three subject areas to N.Terrill (UMIST), L.Pope (Keele) and R.Lewis (DL).

Andy Hammersley described the crystallographic binary file format and a proposal to adopt an imageNCIF file format as the new standard. Richard Denny (Daresbury & Imperial College) described the new graphical user interface, XFIT, for the 1-D peak fitting program and also the latest modifications to LSQINT. John Squire (Imperial College) then showed how he and his group were using LSQINT to extract intensities in the quest to model the first frame of “Muscle: the movie” and how Fourier synthesis would be used to generate the latter frames. David Hukins (Aberdeen) rounded off the day with the second keynote presentation with an intriguing view into the mechanical properties of collagen in the intervertebral disk of the spine. The second day was concluded with a sherry reception and conference dinner at Daresbury.



Photographs

John Squire presenting cheques to the 3 poster prize winners (top right & centre right). Among the scenes captured during the poster session, Tony Ryan demonstrates, to Liz Towns-Andrews, that life isn't so bad with only one good arm (top left). Patrick Fairclough asks John Pople how to dunk his strange looking biscuit (bottom right).

The final day started with our third keynote speaker, Rick Millane (Purdue), who gave a detailed account of both uncorrelated and correlated disorder in polycrystalline fibres. Steve Maginn (MSI) gave a visual demonstration of the capabilities of the Cerius² computer program for both neutron and electron scattering, powder, crystalline or amorphous data. Chick Wilson (Rutherford) outlined his approach to Laue data collection on the SXD time of flight diffractometer at the ISIS facility. Peter Purslow (Royal Veterinary, Denmark) described his current work on the elasticity of fibrillin, a major component of elastic microfibrils. Tim Wess (Stirling) told us about his modelling work on the

structure of collagen and Nageena Malik (OU) continued the theme by telling us about stroma collagen, glycation and the preventative attributes of analgesics, especially aspirin. Neville Greaves (Daresbury) explained how simultaneous SAXS/XAFS/XRD could be used to probe the disorder-order transitions of cordierite glass ceramics. Helen Gleeson (Manchester) presented some recent results from liquid crystal studies using simultaneous SAXS/WAXS/RAMAN/DSC and how each technique can be used to probe a separate feature of the structure. Gordon Tiddy (Salford/Unilever) concluded the session by describing how shear and stopped-flow could be used to study the structure and kinetics of liquid crystals.

The workshop concluded with a special vote of thanks to Janet Smith and Diane Travis for all the hard work and organisation that went into making the whole meeting run smoothly.

A fuller account of the talks/posters presented at this workshop may be read later in this volume or viewed on the World Wide Web at:

<http://www.dl.ac.uk/SRS/CCP13/workshop96>.

Geoff Mant

Synchrotron Radiation Summer School 1996, Italy

In October, 1996 a Summer School on 'Applications of Synchrotron Radiation in Life Sciences and Chemistry' was held at Maratea, Italy. Included as part of this were sessions on Fibre Diffraction given by Trevor Forsyth, Richard Denny and myself. The School was sponsored by the European Synchrotron Radiation Society (ESRS) and was organised by Malcolm Cooper (Warwick), Dominique Maes (Brussels) and Lorenzo Avaldi (Rome). About 50 students and 24 teachers participated in what proved to be a highly successful Workshop. Participants came from all over Europe (Italy, Portugal, France, UK, Germany, Belgium, Finland, Sweden, Denmark, Poland), and also from the US (Boston and Las Vegas). The School was held at the magnificent Hotel Villa del Mare in Maratea, which is on the west coast of southern Italy. For me a four hour train journey south from Rome, was followed by an 'interesting' minibus ride in the dark around a tortuous coastal route with many hairpin bends and a driver who must have been late for his supper. However, having arrived safely, I discovered that the

Hotel had a magnificent site, overlooking the sea close to Sapri, and that it was built into a sheer cliff down to the sea. The lecture room even had the exposed cliff face as one wall. Each level of the Hotel had creeper-hung veranda's, one of which can be seen in the photograph, and breathtaking views. Although it was a 'summer' school, it was obviously at the end of the season. The weather was not brilliant, but when an opportunity presented itself a number of hardy souls (not including me!) took the hotel lift down through the cliff to the private beach below and ventured into the sea. Others enjoyed swimming in the Hotel pool, although the only pool that I got near was the sort that happens on a baize-covered table with balls and a cue. The weather was actually very rough sometimes and the spray and water plumes emanating from the breakers crashing against the rocks surrounding the private beach were quite dramatic and very noisy.

I was involved in the School in three capacities. The first was to teach some basic biology to the students,



most of whom turned out to be chemists or physicists. The second was to provide an introduction to the theory of fibre diffraction, mainly helical diffraction, which was followed up by Richard Denny (Daresbury & Imperial College) on the effects of different kinds of disorder on helical diffraction patterns, and by Trevor Forsyth (Keele) on fibre diffraction from DNA. The third was to present an evening lecture on my own research topic, namely fibre diffraction studies of muscle. Richard and Trevor were also involved in setting up and running tutorial sessions on fibre diffraction, including hands-on experience of running some of the CCP13 programs. The students appeared to appreciate all of our efforts and it was a splendid opportunity to present our subject to a new generation of Synchrotron users. The School also provided an opportunity for us teachers to learn from each other. Not only were there some splendid talks, for example by Professor Malcolm Cooper on 'What is a photon? A cautionary historical tale', by Professor P. Suortti (ESRF) on 'Synchrotron Radiation in Medicine - Angiography' and by Professor G. Margaritondo (Lausanne) on 'Photoelectron Spectroscopy of Biological Materials', to name but three, but I personally enjoyed very much the tutorials on protein crystallography methods given by Fritjof Korber (Liverpool) and by Gerard Kleywegt (Uppsala - who also, wittily, tried to teach us how to pronounce Å correctly - roughly 'ongstrerm'). All of the lecture notes were copied and collated for all participants and we each now have a very good 'hardcopy' overview of the uses of Synchrotron Radiation.

Apart from the formal scientific sessions, such Workshops are also an excellent way for people from different Countries and backgrounds to meet and to discuss their work in an informal way, sometimes over excellent Italian food (although my daily intake of kalamari -something I do not normally eat - was almost as great as that of the local white wine). Two very memorable social events come to mind. One was an evening of local traditional folk music and dance which was very delightful and the other was an excursion to the ruined city of Pompeii. Not only was the weather excellent on that day, but the place itself was amazing and well worth a visit. Amongst the most amazing things still to be seen are some of the original plumbing from a few years AD and some of the artwork on the walls of the houses. And, no, this artwork is not primitive. The use of perspective was impeccable and the images were very realistic. How did man then forget how to do it for centuries afterwards? It was a real eye-opener and showed how the culture of a very advanced civilisation, in housing, plumbing, central heating, architecture and art, can be lost and forgotten, only to be rediscovered centuries later. Pompeii even had traffic (chariot) control systems, pedestrian areas, supermarkets with special out of sight loading bays and street-corner pubs. So what's new? Well, no, they didn't have synchrotrons or fibre diffraction!

John Squire.

CCP13 Program Updates

CCP13 Program Updates

Richard Denny

Biophysics Section, Blackett Laboratory, Imperial College,
London SW7 2BZ &
CCLRC Daresbury Laboratory, Warrington WA4 4AD.

LSQINT

A flexible orientation distribution function (ODF) has been built into the spot profile calculation which has meant that a single profile type now supersedes the four profile types previously available. The ODF has the form,

$$N(\phi) = \frac{k}{\left[1 + 2 \left(\frac{1 - \cos \phi}{\tan^2 \frac{1}{2} \Delta\phi} \right) (2^{1/m} - 1) \right]^m}$$

where k is a normalising constant, $\Delta\phi$ is the width of the distribution and m is a shape factor. The function is similar to a Pearson VII: when $\Delta\phi$ is small, if $m = 1$, the ODF is approximately Lorentzian but as m increases, the ODF becomes more Gaussian in character.

The facility has been added to fit intensity on an image arising from more than one lattice. This is useful when two uncorrelated structures contribute to the same diffraction pattern.

The program FTOREC has long been able to output images remapped into polar coordinates in reciprocal space as well as an estimate of the standard deviations arising from the quadrant folding of the diffraction pattern. LSQINT is now able to use both these files: patterns can be fitted in polar coordinates and the standard deviation file can be used to calculate weights to be used in the fitting procedure. Other modifications include minor bug fixes and the correction of the helical selection rule facility which enabled the number of sampling points on a layer line to be limited by taking into account the helical symmetry.

Graphical user interfaces

Users of software have become accustomed to the pleasing simplicity of using flexible, intuitive and

robust graphical user interfaces (GUIs) for all types of application. Two CCP13 programs, FIT and FIX, seemed to merit the work involved in developing GUIs as their use involves an important interactive element.

The GUIs have been developed using the Motif widget set and the UIM/X interface builder which provides a rapid way of outlining the look of a GUI and many facilities for producing and maintaining the considerable quantity of code required for the modern GUI.

FIT and XFIT

XFIT is the name of the interface program which communicates with FIT (see figure 1) although FIT can still be run in the conventional manner. An "Auto" feature has been added to FIT (which is reflected in XFIT). This enables the user to fit a large number of sequential frames of data without further interaction, having obtained a satisfactory fit to the initial frame. The program proceeds by using the final parameter set for the previous frame as the starting set for the current frame. If the goodness of the fit worsens greatly between consecutive frames, the automatic run is interrupted and the user is asked if the current frame should be reassessed in the interactive mode, the automatic run continuing thereafter. Currently, XFIT is only available at Daresbury to NCD users but it will shortly be available via the CCP13 WWW pages.

FIX and XFIX

Similar in manner to XFIT, XFIX is an interface program designed to communicate with FIX (see figure 2). However, all the graphical functions concerned with analysing the image now reside in XFIT, so that FIX cannot be run independently in its most recent version. New features added to FIX include the capability to produce radial and azimuthal scans of the image which can then be processed in the peak fitting facility of the program. This facility uses many of the interfaces developed for XFIT. XFIX will shortly be made available to NCD users at Daresbury.

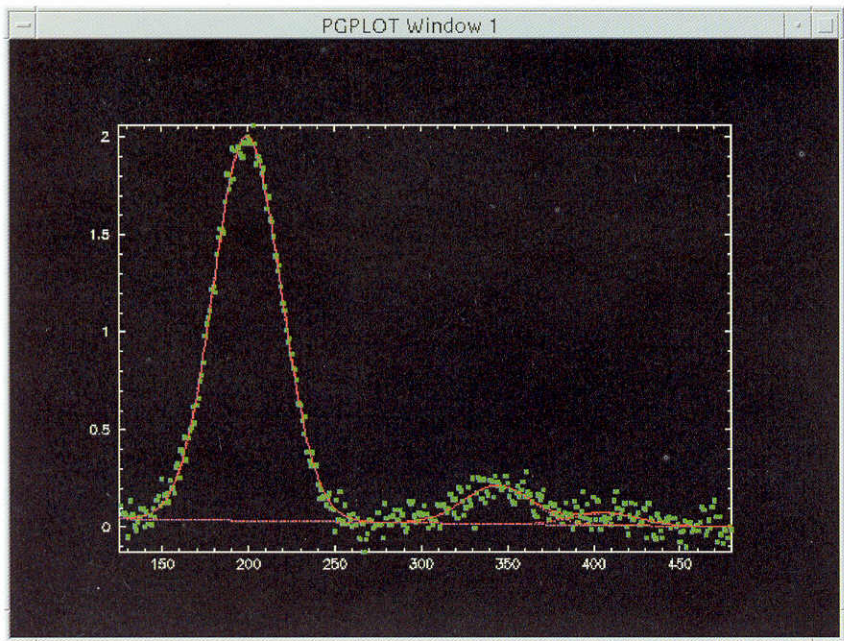


Figure 1: The Setup interface, PGPlot graphics window and Confirm Action dialogue box, displayed while running XFIT. The Setup interface is used to modify parameter values, apply constraints to parameters (through the use of the option menus associated with each parameter in the fit) and to step through the fitting procedure. In the example shown, the widths of the three Gaussian peaks are constrained to be equal, removing two parameters from the fit. If the final solution is unsatisfactory, it is always possible to try again.

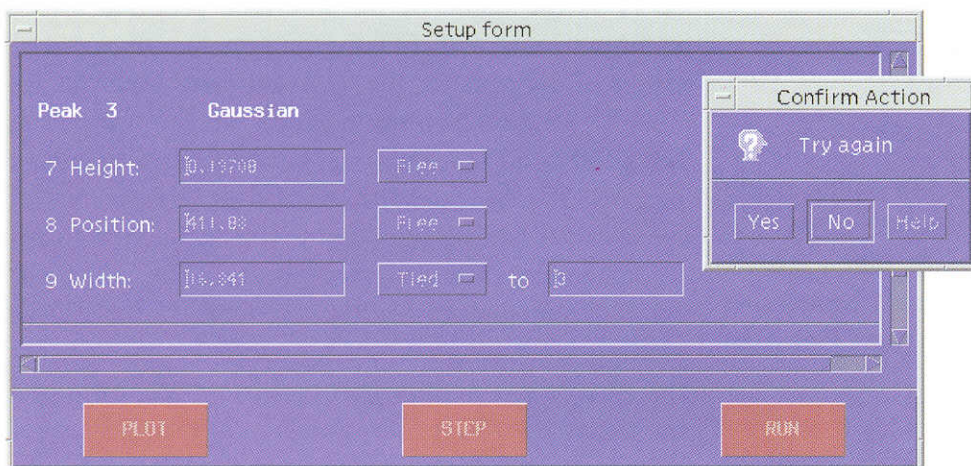
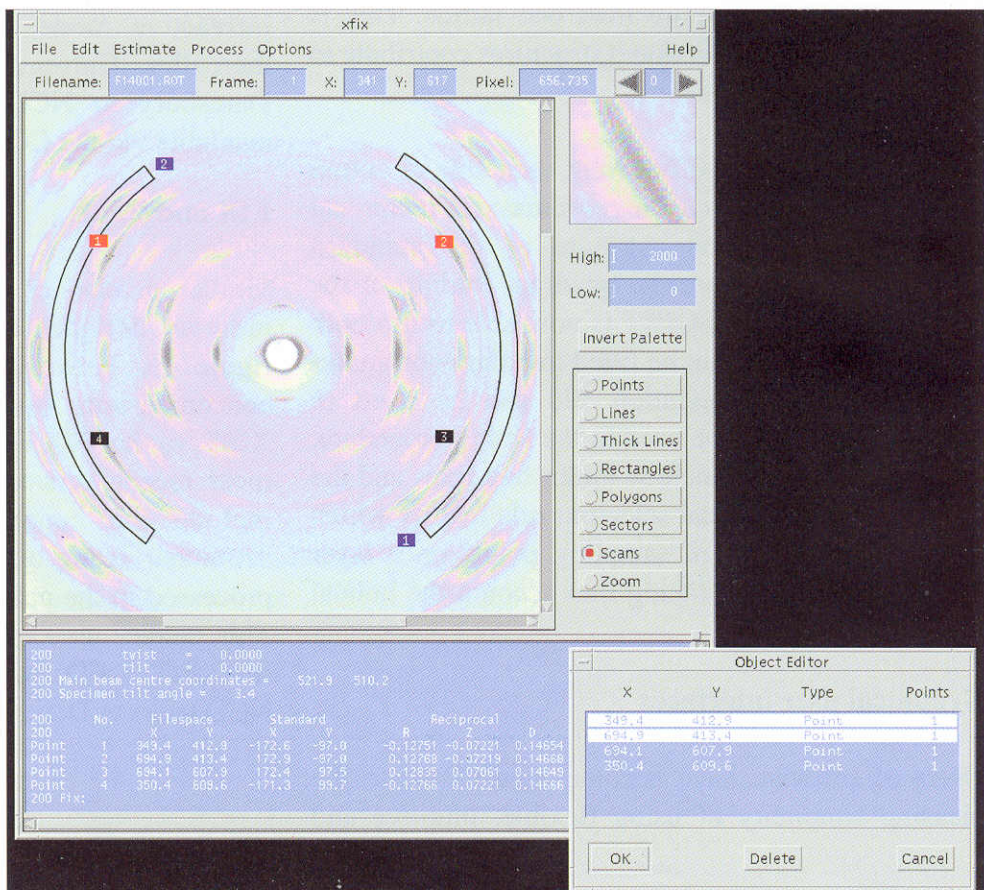


Figure 2: The XFIT interface is shown demonstrating the scan facility (scans are labelled 1 and 2 on a blue background) and the Object Editor. The scans can be integrated across their radial or azimuthal ranges and processed using the peak fitting option. The editor interface has been used to select two points (normally labelled with a black background but highlighted with red). The two selected points could then perhaps be used to estimate the rotation of the pattern.



Summary of Available CCP13/NCD Software

Program	Description
XOTOKO	1-D data manipulation
BSL	2-D data manipulation
v2A	vax to unix data conversion
A2V	unix to vax data conversion
OTCON	ascii to otoko data conversion
RECONV	otoko to ascii data conversion
TIFF2BSL	image plate (tiff) to bsl conversion
I2A	ieee to ansi data conversion (DEC only)
CONV	file format conversion
CORFUNC	correlation function
FD2BSL	intensity to bsl conversion
FDSCALE	scaling and merging of intensities
FIT/PGFIT	1-D fitting and plotting
FIX/PGFIX	preliminary fibre pattern analysis
FTOREC	reciprocal space transformation
LSQINT	2-D integration and background fitting
SAMPLE	Fourier-Bessel smoothing
XFIT	graphical user interface for fit

The tables list the currently distributed CCP13/NCD programs, available as executable modules. The dates refer to the last creation of the executable. HP-UX version 10 executables should be available shortly.

Program	Solaris 2.5	Irix 5.4	Hp-UX 8.0	IBM AIX	Ultronix	OSF	Linux
XOTOKO	14/11/96	30/05/96	27/06/92	-	13/04/92	-	-
BSL	31/05/96	11/06/96	27/06/92	-	13/04/92	-	-
v2A	19/05/96	-	27/06/92	-	13/04/92	-	-
A2V	19/05/95	-	-	-	-	-	-
OTCON	06/06/95	08/07/94	-	-	-	-	-
RECONV	06/06/95	31/10/94	28/06/92	-	-	-	-
TIFF2BSL	06/06/95	-	-	-	-	-	-
I2A	n/a	n/a	n/a	n/a	09/10/92	-	-
CONV	05/11/96	04/11/96	05/04/95	18/05/95	04/11/96	04/11/96	04/11/96
CORFUNC	26/10/95	-	-	-	-	-	-
FD2BSL	05/11/96	04/11/96	01/12/95	18/05/95	04/11/96	04/11/96	04/11/96
FDSCALE	05/11/96	04/11/96	01/12/95	18/05/95	04/11/96	04/11/96	04/11/96
FIT/PGFIT	22/01/97	05/11/96	-	-	23/01/97	-	-
FIX/PGFIX	05/11/96	04/11/96	29/11/95	18/05/95	04/11/96	04/11/96	04/11/96
FTOREC	05/11/96	04/11/96	01/12/95	11/07/95	04/11/96	04/11/96	04/11/96
LSQINT	05/11/96	04/11/96	27/10/95	18/05/95	04/11/96	04/11/96	04/11/96
SAMPLE	05/11/96	04/11/96	01/12/95	24/05/95	04/11/96	04/11/96	04/11/96
XFIT	22/01/97	-	-	-	-	-	-

Contributed Articles

Collagen Fibril Orientations in Tissues and their Relationship to Mechanical Properties

David W.L. Hukins

Department of Bio-Medical Physics and Bio-Engineering,
University of Aberdeen, Foresterhill, Aberdeen AB15 2ZD,
Scotland.

Phone: 01224 681818 ext 53495
Fax: 01224 685645
E-mail: d.hukins@biomed.abdn.ac.uk

Introduction

Collagen fibrils provide tensile reinforcement to the extracellular matrix (ECM) of tissues. The mechanical properties of connective tissues, such as tendon, cartilage etc., depend on their ECM being able to withstand appreciable applied forces. These forces may be generated by the musculature or be externally applied. Collagen molecules are rod-shaped and packed together to form fibrils which are stabilised by intermolecular covalent cross-links. Thus the fibrils are stiff and strong when they are subjected to axial tension but have little flexural, torsional or compressive stiffness, except in hard tissues like bone where the mineral phase modifies the properties of collagen.

Therefore, collagen fibrils can reinforce soft tissues provided that they are oriented in the directions in which tensile stress is generated. Thus the ECM is a biological example of a fibre-reinforced composite material. However, many tissues have to withstand compression, torsion and flexion as well as tension. Collagen fibrils can still provide reinforcement provided they are oriented so that they are placed in tension when the tissue is loaded. Provided the directions in which the fibrils are oriented can be measured experimentally, the results can be identified with the directions in which the tissue can withstand tensile stress and used to formulate models for the mechanical stability of tissues. This approach has been applied to understanding the mechanical stability of articular cartilage [1], the meniscus of the knee joint [2], the urethra [3], the intervertebral disc [4], spinal ligaments [5] and the uterine cervix [6]. More recently, it is being used to investigate the structural basis of creep and stress relaxation in ECM [7].

Determination of fibril orientation

The most convenient method for determining the orientation of collagen fibrils in a tissue site is from a single high-angle X-ray diffraction pattern. The method depends on the ability to obtain a tissue sample, which may be a section cut for the purpose, in which the preferred orientation of the fibrils is in a plane perpendicular to the X-ray beam. The equator of the diffraction pattern then defines the perpendicular to the preferred orientation and the angular spread of the equatorial intensity maxima depends on the orientation distribution function, $g(\phi)$, defined to be the probability of finding a fibril oriented between ϕ and $\phi + d\phi$ with respect to the preferred orientation [8].

If $I(\phi)$ is the angular distribution of equatorial intensity from a perfectly oriented sample (a dogfish fin-ray), then the corresponding intensity distribution from an imperfectly oriented assembly of fibrils is given by

$$I_s(\phi) = g(\phi) * I(\phi)$$

where $*$ represents convolution. The most convenient means of recovering $g(\phi)$ from experimental measurements of $I(\phi)$ and $I_s(\phi)$ is to express them as sums of even-ordered Legendre polynomials [8] of the form

$$I(\phi) = \sum_{n=0}^{\infty} (n+1/2) \langle P_n \rangle P_n(\cos\phi)$$

where the summation is over sufficient even orders of n to reproduce the experimentally determined form of $I(\phi)$ and $\langle P_n \rangle$ are empirical coefficients required to obtain a satisfactory fit. The Legendre polynomial $P_n(\cos\phi)$ is completely defined in the range $0 \leq \phi \leq 2\pi$ and can be computed using the Rodrigues'

$$P_n(x) = \sum_m^M (-1)^m (2n-2m)! x^{n-2m} / \{ 2^n m! (n-m)! (n-2m)! \}$$

formula

where $M = n/2$ for n even. Values of $\langle P_n \rangle$ can be computed from the experimentally determined $I(\phi)$

$$\langle P_n \rangle = \int_0^\pi I(\phi) P_n(\cos\phi) \sin\phi d\phi / \int_0^\pi (\phi) \sin\phi d\phi$$

by

The orientation distribution function, $g(\phi)$, may then

$$g(\phi) = \sum_{n=0}^{\infty} (n + 1/2) \langle P_n \rangle_g P_n(\cos\phi)$$

be computed from

$$\langle P_n \rangle_g = \langle P_n \rangle_s / \langle P_n \rangle$$

where

Here $\langle P_n \rangle_s$ are the empirical coefficients determined from $I_s(\phi)$, the angular intensity distribution from the tissue site, and $\langle P_n \rangle$ are determined from $I(\phi)$, the intensity distribution from the fin-ray.

Compression of the intervertebral disc

The response of the intervertebral disc to compression will be used to illustrate how collagen fibril orientations can be used to formulate models for tissue stability and how such models may be tested experimentally. The intervertebral disc forms a flexible coupling between the vertebrae of the spine [4]. It is roughly cylindrical and has a soft centre, the nucleus pulposus, in which the collagen fibrils are apparently randomly oriented. The nucleus pulposus is surrounded by the annulus fibrosus which consists of a series of coaxial lamellae. In a single lamella the collagen fibrils are highly oriented at an angle of about 65° with respect to the axis of the spine; the direction of tilt alternates in successive lamellae. Figure 1 shows a schematic diagram of a single collagen fibril in a single lamella. The fibril has length, L, tilt, θ , and azimuthal span, ω radians. The lamella has height, h, and radius, r, and encloses a

$$V = \pi r^2 h = \pi [(L/\omega) \sin \theta]^2 L \cos \theta = (\pi/\omega^2) L^3 \sin^2 \theta \cos \theta$$

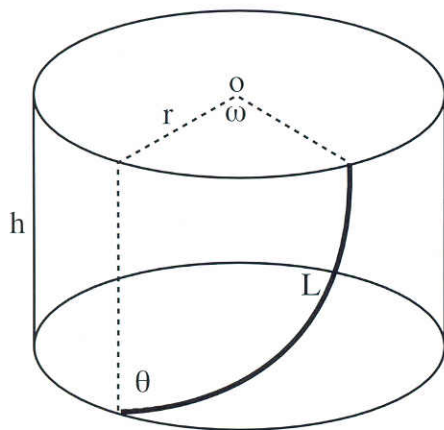


Figure 1. Schematic diagram of the path of a single collagen fibril (bold) in a lamella of the annulus fibrosus of the intervertebral disc. The lamella is modelled as a cylinder of radius, r , and height, h , whose upper face is centred at O . Then ω is the azimuthal span of the fibre which is also characterised by a tilt, θ , and length, L .

volume

$$\delta V = (\partial V / \partial L) \delta L + (\partial V / \partial \theta) \delta \theta$$

$$= 3(\pi / \omega^2)(L^2 \sin^2 \theta \cos \theta) \delta L + (\pi / \omega^2)L^3(2 \sin \theta \cos^2 \theta - \sin^3 \theta) \delta \theta$$

$$\Rightarrow \delta V / V = (3/L)\delta L + (2 \cos^2 \theta - \sin^2 \theta) \delta \theta / (\sin \theta \cos \theta)$$

For pure compression, ω remains constant, and for compression at constant volume, $\delta V/V = 0$. If the collagen fibrils are subjected to a tensile stress, they will acquire a tensile strain so that $\delta L/L > 0$. This condition will be satisfied if $\sin^2 \theta > 2 \cos^2 \theta$, i.e. if $\theta > 54.7^\circ$.

Since experiment shows that $\theta \approx 65^\circ$, the collagen fibrils are strained when the disc is compressed, i.e. the fibrils provide effective tensile reinforcement. If radius is constant, simple geometry also shows that when the disc is compressed and the fibrils are strained, the value of θ increases from its initial

$$\theta = \tan^{-1}[(h_0/h) \tan \theta_0]$$

value, θ_0 , to

where h_0 is the initial value of the disc height, h . This relationship has been used to test the theory of the response of the collagen fibril network of the annulus fibrosus to compression of the intervertebral disc; a fully hydrated intact rabbit disc was compressed in stages and X-ray diffraction patterns were recorded at each stage to show that the fibre tilt increased as predicted [9]. More complicated finite element models show how the annulus fibrosus bulges as the disc is compressed [10]. In the living spine, the disc is often subjected to offset compression which leads to bending. Magnetic Resonance (MR) images of human volunteers then shows that the nucleus pulposus shifts within the disc [11].

Viscoelasticity

High-angle diffraction patterns from connective tissues have usually been obtained using conventional X-ray sources. In some experiments the tissue has been subjected to a series of fixed strains. A diffraction pattern has then been obtained from each strained state with a typical exposure time of about 30min. However, most tissues are viscoelastic. For example, the viscoelastic properties of both the intact intervertebral disc [12] and the nucleus pulposus [13] have been established. A viscoelastic material dissipates some of its strain energy. Since any dissipation process has a finite relaxation time, the stiffness of a viscoelastic material decreases with decreased loading rate. Thus, when a tissue is

subjected to a fixed strain, the stress within the tissue decreases, *i.e.* it experiences stress relaxation. Similarly, when a tissue is subjected to a fixed stress its strain will continue to increase, *i.e.* it exhibits creep.

Recent experiments have used synchrotron radiation to investigate the orientation of collagen fibrils in skin and perimysium (muscle connective tissue) [7]. In both tissues, the initial application of load leads to fibrils tending to reorient in the direction of applied load. However, there was no detectable change in fibril orientation during either creep or stress relaxation. These results indicate that simple geometric models are inadequate to explain the viscoelastic properties of ECM. This result is expected for stress relaxation, where the overall dimensions of the tissue do not change, and is consistent with X-ray diffraction patterns of intervertebral disc [4] and ligaments [5] showing fixed fibril orientations over a period of about 30 min at fixed strains. However, the results of creep experiments are more surprising and merit further investigation.

Preliminary experiments are also being performed on the response of the collagen fibril network of uterine cervix to creep (in collaboration with Mr S.J.Wilkinson). These experiments are being performed on rat tissue which provides an established model for the changes which occur in the human cervix during labour [6]. The creep rate of the cervix increases at term, allowing it to dilate so that the neonate can pass through. Furthermore, this change in mechanical properties is accompanied by a change in NMR relaxation times [14] which may explain the changes apparent in MR images of human patients. Understanding the relationship between structure and mechanical properties of the rat cervix may then be a step in relating the appearance of the human cervix in MR images to its properties and, hence, to the diagnosis of a cervix which changes its mechanical properties too early in pregnancy or not at all.

References

- [1] D.W.L. Hukins, R.M. Aspden. In *Material Properties and Stress Analysis in Biomechanics*, A.L. Yettram (ed.), pp. 44-59, Manchester University Press, Manchester, 1989.
- [2] R.M. Aspden, D.W.L. Hukins. In *Material Properties and Stress Analysis in Biomechanics*, A.L. Yettram (ed.), pp. 109-122, Manchester University Press, Manchester, 1989.
- [3] D.S. Hickey, J.I. Phillips, D.W.L. Hukins. *British Journal of Urology* **54**, 556-561 (1982).
- [4] D.W.L. Hukins. In *Biology of the Intervertebral Disc*, vol. 1, P. Ghosh (ed.), pp. 1-37, CRC Press, Boca Raton, 1988.
- [5] D.W.L. Hukins, M.C. Kirby, T.A. Sikoryn, R.M. Aspden, A.J. Cox. *Spine* **15**, 787-795 (1990).
- [6] R.M. Aspden. In *Connective Tissue Matrix*, part 2, D.W.L. Hukins (ed.), pp. 199-228, Macmillan, London, 1990.
- [7] P.P. Purslow, D.W.L. Hukins. International Biomechanics Conference, Amsterdam, 1994.
- [8] M.C. Kirby, R.M. Aspden, D.W.L. Hukins. *Journal of Applied Crystallography* **21**, 929-934 (1988).
- [9] J.A. Klein, D.W.L. Hukins, *Biochimica et Biophysica Acta* **717**, 61-64 (1982).
- [10] K.J. Mathias, J.R. Meakin, A. Heaton, M.W. Brian, S. Mierendorff, R.M. Aspden, J.C. Leahy, D.W.L. Hukins. In *NAFEMS World Congress*, in press.
- [11] A.J. Fennell, A.P. Jones, D.W.L. Hukins. *Spine*, in press.
- [12] A.D. Holmes, D.W.L. Hukins. *Medical Engineering and Physics* **18**, 99-104 (1996).
- [13] J.C. Leahy, D.W.L. Hukins. *Journal of Back and Musculoskeletal Rehabilitation*, in press.
- [14] J. Blacker, M.A. Foster, R.M. Aspden. British Institute of Radiology Meeting, Birmingham,

Diffraction by Disordered Fibres

R. P. Millane and W. J. Stroud

Whistler Center for Carbohydrate Research and Computational Science and Engineering Program, Purdue University, West Lafayette, Indiana 47907-1160, U.S.A.

Introduction

Diffraction patterns from some polycrystalline fibres contain sharp Bragg reflections at low resolution, giving way to continuous layer line intensities at high resolution [1,2]. Such specimens are essentially polycrystalline, but the packing of the molecules in the crystallites is disordered. Accurate structure

determination using data from such diffraction patterns requires that the effects of disorder on the diffracted intensities be included in a rigorous manner. Towards this end, we have developed models of disordered polycrystalline fibres and their diffraction properties [3-7], which we summarise here.

The approach we adopt involves construction of statistical models of disordered crystallites, and calculation of resulting diffraction patterns. Disorder is described in terms of probability density functions that describe perturbations of the crystalline structure away from ideal order, and the diffraction from a fibre is calculated as an ensemble average over the imperfect crystallites. An alternative approach is to build representative crystallites based on appropriate intermolecular potentials and average the diffraction over many such realisations. Although this approach may be useful for some simple systems, for more complex systems it has the disadvantage that the results depend on knowing the relevant potentials quite accurately, and it is enormously expensive computationally. Our approach is to describe the overall distortions in the crystal lattice (which are the primary determinants of the diffraction) while ignoring the details of the particular interactions that give rise to these. The advantage of this approach is that it is generally applicable, and analytical expressions can be obtained that allow efficient calculation of diffraction patterns.

It is convenient to regard disorder as having two components, referred to as *lattice disorder* and *substitution disorder*. Lattice disorder consists of deviations in the positions of the molecules from those in an average lattice. The molecules are treated as rigid bodies, so that lattice disorder consists of distortions of a two-dimensional lattice into three-dimensional space. Substitution disorder consists of variations in the dispositions of the molecules at each lattice site, which in our case consists of rotations of the molecules about their long axes, and variations in their direction (“up” or “down”). Lattice and substitution disorder are assumed to be independent of each other.

The layer line intensities diffracted from an ensemble of disordered crystallites can be written as

$$I_l(R) = \left\langle \left\langle I(R, \psi, Z = l/c) \right\rangle_d \right\rangle_\psi \quad (1)$$

where $I(R, \psi, Z)$ is the intensity diffracted from a

single crystallite, $\langle \rangle_d$ denotes averaging over all states of disorder, $\langle \rangle_\psi$ denotes cylindrical averaging, and c is the axial repeat distance of the molecules. The problem is then one of constructing appropriate models of a disordered crystallite and evaluating the averages in eq. (1). We have considered two different kinds of models; one of *uncorrelated* disorder, and the other of *correlated* disorder.

Uncorrelated disorder

In the case of uncorrelated disorder, for the lattice disorder we assume Gaussian statistics, that the components of the distortion vectors are independent, and that the variances of components in the ‘lateral’ plane (normal to the fibre axis) are equal. The cylindrically averaged diffracted intensity can then be expressed as the sum of Bragg (B) and diffuse (D) or continuous components [3,4]:

$$I_l(R) = I_l^B(R) + I_l^D(R) \quad (2)$$

The Bragg component consists of sharp reflections whose widths (shapes) depend on the average crystallite size (as well as instrumental effects) and are constant throughout reciprocal space. As a result of the disorder, the magnitude of the Bragg reflections is weighted down with increasing resolution, the weighting function being given by [4]

$$W_{lattice}(R, Z) = \exp(-4\pi^2[R^2\sigma_{lat}^2 + Z^2\sigma_{axial}^2]) \quad (3)$$

where σ_{lat}^2 and σ_{axial}^2 are the variances of the lateral and axial distortions, respectively. The diffuse component consists of the continuous layer line diffraction that would be diffracted by a noncrystalline fibre except that, as a result of the disorder, it is weighted up (by $[1 - w_{lattice}(R, Z)]$) with increasing resolution. The effect of substitution disorder is to weight the different Fourier-Bessel structure factors, $G_{nl}(R)$, by the weighting function

$$W_{nl} = \int_0^{c/l} \int_0^{2\pi} p(\phi, z) \exp[i(2\pi z l / c - n\phi)] d\phi dz \quad (4)$$

where $p(\phi, z)$ is the probability density function for the angular position of a molecule deviating by ϕ , and the axial position deviating by z , from their values in an ordered lattice [4]. A particular kind of disorder is described by a particular $p(\phi, z)$ from which the w_{nl} can be calculated [4]. The effect of rotational disorder is to weight down the contribution of the higher order Fourier-Bessel terms to the Bragg intensity, and to correspondingly increase their

contribution to the diffuse intensity. The larger the variance of the rotational disorder, the more rapidly the weights fall off with Bessel order. For *random rotations*, only the zero-order Bessel term contributes to the Bragg intensity and the non-zero orders contribute to the diffuse intensity. For specimens in which the molecules are *screw disordered* (*i.e.* rotational disorder is coupled to translational disorder), for an integral helix, the contribution of a Fourier-Bessel term to the Bragg intensity is weighted down more with increasing difference between the Bessel order and the layer line index, and the contribution to the diffuse intensity is correspondingly weighted up [4].

The effects of uncorrelated disorder are illustrated in figure 1 which shows the layer line amplitudes $I_l^{1/2}(R)$ for random screw disorder, (a) alone and (b) with lattice disorder, for a molecule with 10-fold helix symmetry [4]. In (a) Bragg reflections are eliminated close to the meridian on the higher layer lines, but persist out to high resolution on all layer lines. The effect of adding lattice disorder is to suppress the Bragg reflections at high resolution as shown in (b). Note the importance of the lattice disorder in suppressing the Bragg reflections at high resolution, a feature that cannot be explained by screw disorder alone.

By calculating diffraction patterns using a molecular structure and the model of disorder described above, and comparing them with measured diffraction patterns, the disorder parameters may be adjusted, in

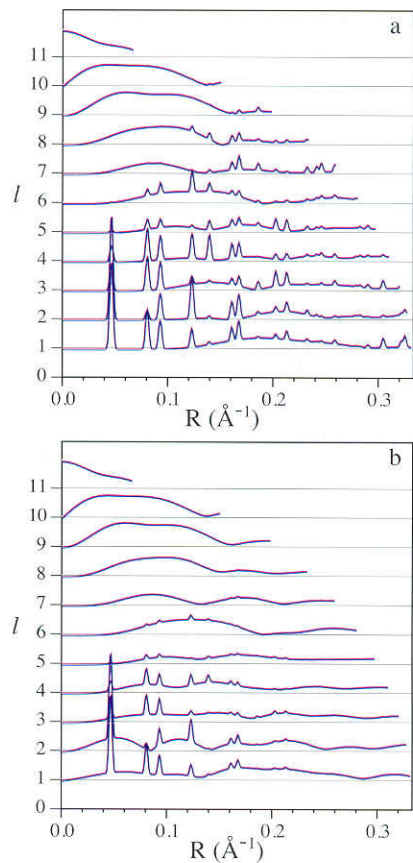


Figure 1:
Calculated layer line amplitudes for a polycrystalline fibre with random screw disorder with (a) no lattice disorder and (b) uncorrelated lattice disorder [4].

an iterative fashion, to optimise the agreement between the calculated and measured patterns [5]. This allows one to identify the kind and degree of disorder in a particular fibre specimen. An example is shown in figure 2 [5]. One quadrant of a diffraction pattern recorded from a polynucleotide (poly(dA)-poly(dT)) fibre is shown in (a), and that calculated from an optimised model (including the effects of coherence length, crystallite size and disorientation) is shown in (b). The resulting model

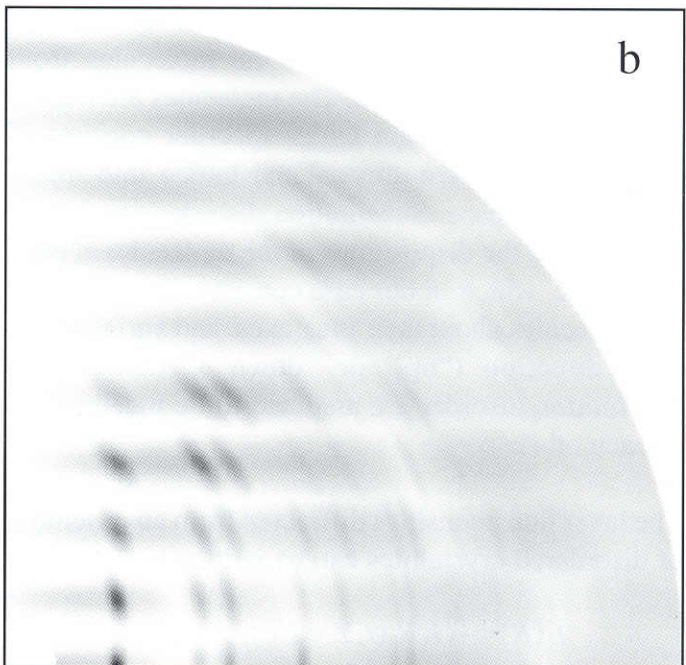
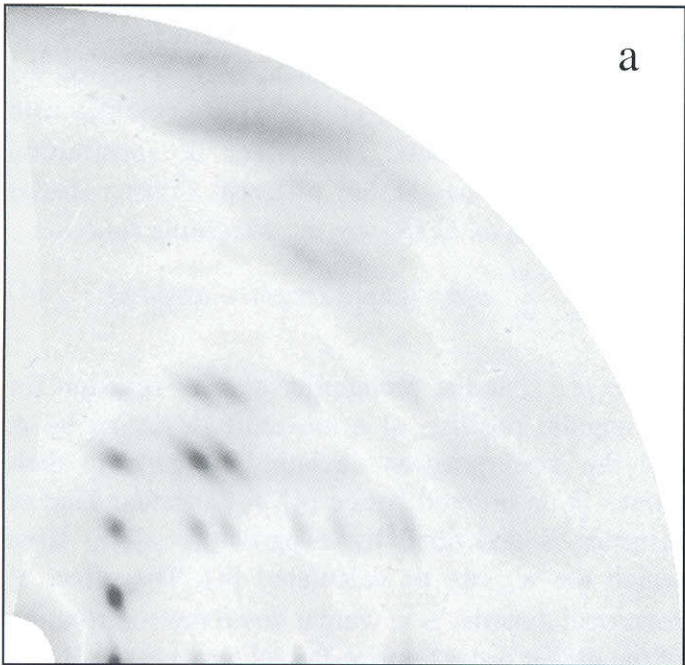


Figure 2: (a) Measured and (b) calculated (with uncorrelated disorder) diffraction patterns, in one quadrant of reciprocal space from a (poly(dA)-poly(dT)) fibre [5].

incorporates random screw disorder and lattice distortions with standard deviations of 0.6\AA^{-1} along the molecular axes and 0.5\AA^{-1} normal to the molecular axes.

Correlated disorder

In a close-packed system such as a crystallite in a polymer fibre, it is probable that distortions at one lattice site will influence the distortions at neighbouring sites. Furthermore, diffraction patterns from some disordered fibres do not appear to consist of distinct Bragg and diffuse components as described above, but contain Bragg reflections that broaden with increasing resolution and blend into the continuous diffraction at high resolution. This is generally considered to result from correlated distortions of the crystal lattice [8,9]. Although there may be correlations between the rotational distortions of neighbouring molecules, these are likely to be weaker and not of a general, simple form. The second model we consider therefore, is one of correlated lattice disorder and uncorrelated substitution disorder. Although the paracrystalline model is often used to describe correlated disorder in polymer crystals [8], we have chosen to use a perturbed lattice model [9] to avoid some of the difficulties inherent in the paracrystalline model [6,7]. We impose a correlation field on the crystal lattice, rather than deriving the correlations from nearest neighbour statistics, as this allows manageable expressions for calculating diffraction patterns to be obtained [6,7].

For the lattice disorder, the components of the distortion vectors are as described above, except that the distortions at neighbouring sites are coupled, the

coupling being described by two exponential correlation fields, one for the lateral distortions and one for the axial distortions. The disorder is then described by lateral and axial variances, and lateral and axial correlation lengths. The degree of order in the lattice decreases as the variance increases, and increases as the correlation length increases. Uncorrelated substitution disorder (as described above) can be incorporated using the weights w_{nl} . Because of the correlations, the diffracted intensity does not separate into two components as in eq. (2), and it is not possible to express it in terms of only reciprocal space quantities. The diffracted intensity must be expressed as a sum over the real space lattice, although considerable analytical simplification is possible that allows efficient computation of the cylindrically averaged intensity

$$I_l(R) = \sum_j w_{jl}(R, r_j) \sum_{m,n} H_{mnl}(R, r_j, \phi_j) \quad (5)$$

[6,7]. The result can be expressed in the form where the sum over j is over the sites of the undistorted two-dimensional lattice within the region of the autocorrelation function of the crystallite, the (r_j, ϕ_j) are the polar coordinates of these sites, the w_{jl} depend on the site variances and correlation lengths, the sum over m and n is over the orders of the contributing Bessel terms, and the H_{mnl} depend on the substitution disorder weights and Fourier-Bessel structure factors [6,7].

Figure 3 shows calculated diffraction patterns that illustrate the effects of correlated lattice disorder for a molecule with 11-fold helix symmetry [7]. The pattern shown in (a) is for a fibre with uncorrelated axial lattice disorder only, which has the effect of introducing diffuse intensity on the upper layer lines

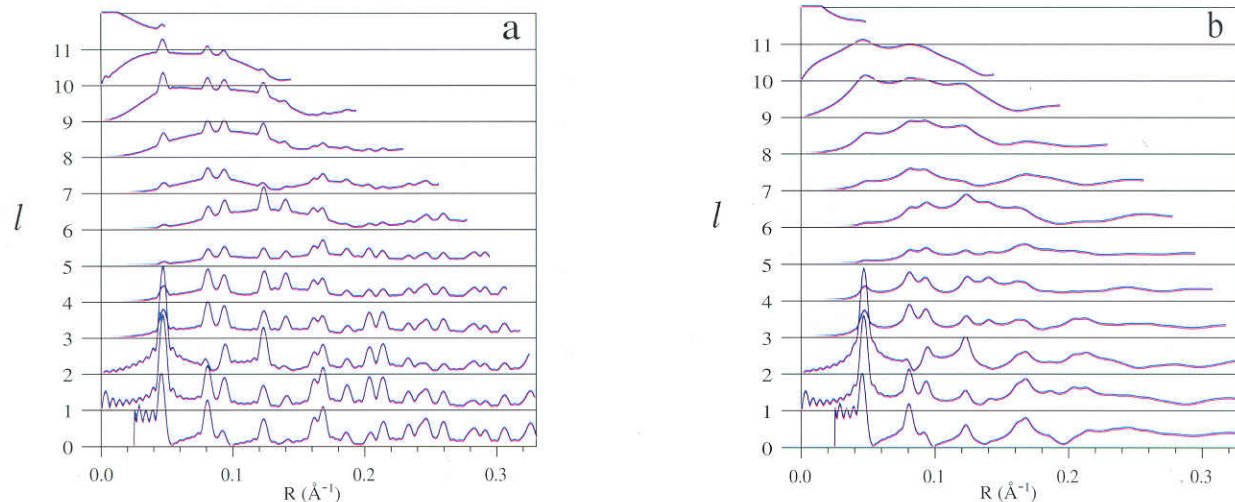


Figure 3: Calculated layer line amplitudes for a polycrystalline fibre with (a) uncorrelated axial lattice disorder, and (b) correlated lateral and axial lattice disorder [7].

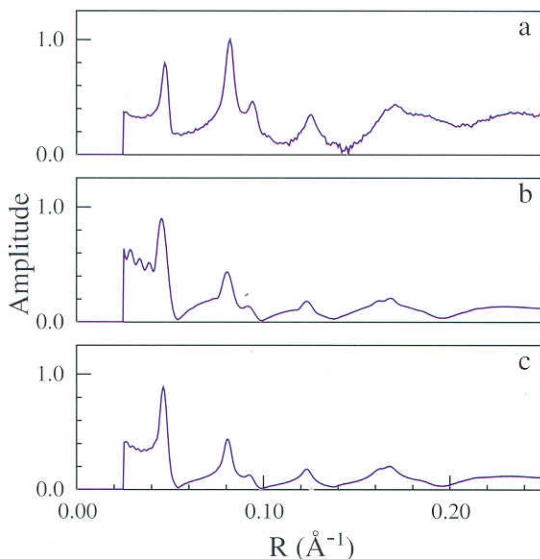


Figure 4: Equatorial diffracted amplitude, (a) measured from a (poly(dA)·poly(rU)) fibre, (b) calculated for uncorrelated disorder, and (c) calculated for correlated disorder [7].

with superimposed Bragg reflections of invariant width. The pattern in (b) shows the effects of correlated lateral and axial lattice disorder; the Bragg peaks broaden with increasing resolution and blend into the diffuse diffraction, and the pattern no longer has the appearance of a Bragg component superimposed on a continuous component.

As in the case of correlated disorder, comparison of diffraction patterns calculated using the model of correlated disorder with measured patterns may be used to characterise correlated disorder in a fibre specimen. Figure 4 shows the results of such a calculation [7]. The diffraction pattern from a polynucleotide (poly(dA)·poly(rU)) fibre shows evidence of correlated lateral lattice disorder since the Bragg reflections on the equator broaden and give way to continuous amplitude with increasing resolution (a). The best fit to the measured equatorial diffraction using a model of uncorrelated disorder (corrected for the effects of disorientation, coherence length, and instrumental broadening) is shown in (b). Although the calculated pattern matches most of the features of the observed pattern, it produces shoulders on the Bragg reflections, and Bragg reflections of constant width, neither of which are consistent with the data, and both indicating the presence of correlated disorder. A diffraction pattern calculated from an optimised model containing correlated lateral lattice disorder is shown in (c), and is seen to significantly reduce the discrepancies noted above. In this case, the lateral variance and correlation length are 1.9 Å and 125 Å, respectively.

Conclusions

We have developed two rather general models of disordered polycrystalline fibres that allow efficient calculation of diffraction patterns. The model of uncorrelated lattice disorder and uncorrelated substitution disorder is formulated in reciprocal space and appears to explain most of the features seen in diffraction patterns from some disordered fibres. The second model includes correlated lattice distortions (which are expected to be present to at least some degree), is formulated in real space, and appears to explain peak broadening seen in diffraction patterns from some fibres. Both models are quite flexible, and parameters describing the disorder can be adjusted to optimise the models against fibre diffraction data.

Supported by the U.S. National Science Foundation (MCB-9219736)

References

- [1] A. Miller and D.A.D. Parry, A review of statistical structures in polypeptides and biological macromolecules, *Polymer*, **15**, 706-712 (1974).
- [2] S. Arnott, Twenty years hard labour as a fibre diffractionist, in *Fibre Diffraction Methods*, A.D. French and K.H. Gardner (eds.), ACS Symposium Series, Vol. 141, 1-30, 1980.
- [3] R.P. Millane and W.J. Stroud, Effects of disorder on fibre diffraction patterns, *Int. J. Biol. Macromol.*, **13**, 202-208 (1991).
- [4] W.J. Stroud and R.P. Millane, Diffraction by disordered polycrystalline fibres, *Acta Cryst.*, **A51**, 771-790 (1995).
- [5] W.J. Stroud and R.P. Millane, Analysis of disorder in biopolymer fibres, *Acta Cryst.*, **A51**, 790-800 (1995).
- [6] W.J. Stroud and R.P. Millane, Cylindrically averaged diffraction by distorted lattices, *Proc. R. Soc. Lond.*, **A452**, 151-173 (1996).
- [7] W.J. Stroud and R.P. Millane, Diffraction by polycrystalline fibres with correlated disorder, *Acta Cryst.*, **A52**, 812-829 (1996).
- [8] R. Hosemann and S.N. Bagchi, *Direct Analysis of Diffraction by Matter*, North-Holland, Amsterdam, 1962.
- [9] T.R. Welberry, Diffuse X-ray scattering and models of disorder, *Rep. Prog. Phys.*, **48**, 1543-1593 (1985).

Advantages of Absolute Calibration in Small-Angle X-ray and Neutron Scattering Studies of Polymers and Colloids

George D. Wignall

Solid State Division Oak Ridge National Laboratory, Oak Ridge, Tennessee 37931-6393.

The angular distribution of the intensity of scattered radiation (X-rays, neutrons etc.) reflects the structure of the material and is measured as a function of the momentum transfer, $Q = 4 \pi \lambda^{-1} \sin \theta$, where λ is the wavelength and 2θ is the angle of scatter. Because of the inverse (Fourier) relationship between the structure in real-space (D) and the scattering in Q -space ($D \sim 2\pi/Q$), data at lower Q -values probe longer length scales and these measurements are conventionally referred to as **small-angle X-ray or neutron scattering (SAXS and SANS)**, though it is the Q -range which determines the length scale probed (typically $\sim 10\text{-}1000\text{\AA}$). This paper emphasizes the importance of placing such data on an absolute scale, in the form of a differential cross-section $d\Sigma/d\Omega(Q)$, per unit sample volume (in units of cm^{-1}). The use of absolute units is not essential for the measurement of spatial dimensions, though it forms a valuable diagnostic tool for the detection of artifacts, to which scattering techniques are particularly vulnerable. Because the cross section varies as the sixth power of the dimensions [1], it is a very sensitive indicator of whether an appropriate structural model has been chosen. Absolute calibration allows artifacts to be recognized, and the model parameters may be restricted to those which reproduce the observed cross-section, as illustrated in the following examples.

Example 1: SANS and SAXS from melt crystallized polyethylene

Figure 1a shows a Zimm plot [$(d\Sigma/d\Omega)^{-1}$ vs. Q^2] of the SANS data from 6.0wt.% of deuterated polyethylene (PED) in a matrix of unlabeled PEH after rapidly quenching from the melt. The signal arises from the difference in scattering length between H^1 and D^2 nuclei, so that deuterated and protonated molecules have strong neutron scattering contrast. The extrapolated cross-section [$d\Sigma/d\Omega(0) \approx 28.0 \text{ cm}^{-1}$] is proportional to the molecular weight (MW) and when the sample is rapidly quenched (crystallized) from the melt, the SANS data lead to $MW \approx 45,000$, which is of the same order as the value from chromatography [4]. However, when the

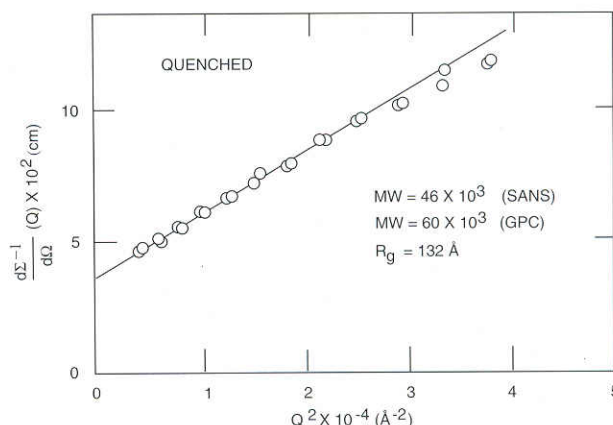


Figure 1a: Typical Zimm plot for 6% PED molecules in PEH matrix quenched from the melt.

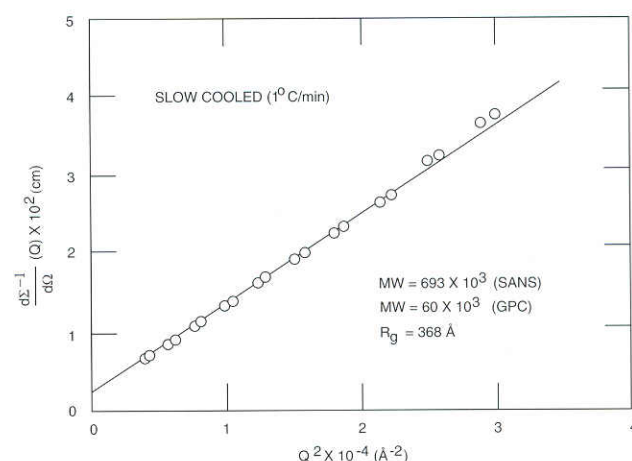
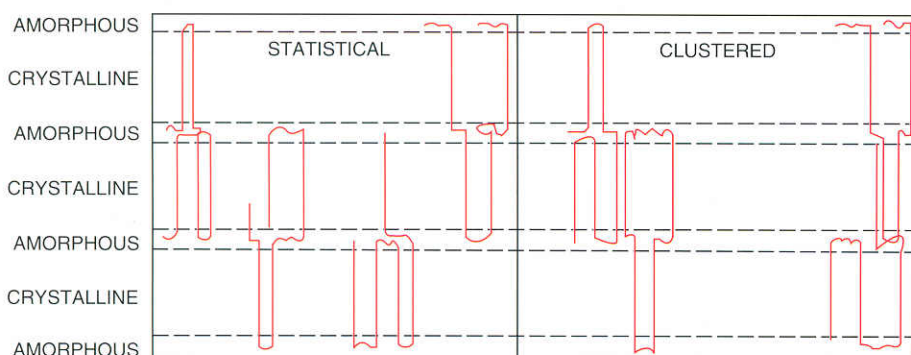


Figure 1b: Typical Zimm plot for 6% PED molecules in PEH matrix slow cooled (1°C/min) from the melt.

same sample is slowly cooled (crystallized) from the melt, figure 1b, the apparent MW increases by over an order of magnitude. It is clear that these data do not originate in the scattering from single molecules, and it has been shown that the excess intensity is caused by aggregation or clustering of the D-labelled molecules [2], due to the difference in melting point ($\sim 5^\circ\text{C}$) between protonated and deuterated species. On slow cooling, the PEH crystallizes first, leading to a non-uniform distribution of PED in PEH as illustrated schematically in figure 2, though rapid quenching does not allow time for such a separation to develop. This artifact would not be apparent if the data were in arbitrary units, thus illustrating the point referred to above, that the intensity is extremely sensitive to the dimensions and even an approximate ($\pm 25\%$) absolute calibration is sufficient to reveal the presence of such inhomogeneities.

In the case of a sample of pure deuterated polyethylene (PED), the signal arises from the density difference between the alternating crystalline and amorphous regions in the lamellar stack, and it

Measure MW VIA CHROMATOGRAPHY (MW-GPC)
AND ALSO VIA SANS (MW-SANS)
MW-SANS ~ MW-GPC (RAPIDLY QUENCHED FROM MELT)
MW-SANS >> MW-GPC (SLOWLY COOLED FROM MELT)



may be shown [5] that the SAXS and SANS cross-sections are virtually identical, apart from a scale factor. Figure 3 shows absolute SAXS and SANS data for the same sample of PED and the theoretical ratio of the two signals (1.27) is in good agreement with the measured ratio (1.31 ± 0.1), thus giving a cross check on the validity of the independently calibrated SAXS and SANS data.

Example 2: Blockcopolymer Micelles in Supercritical Carbon Dioxide

Supercritical CO_2 presents an environmentally benign medium for polymerizations which minimizes the production of organic solvent and aqueous wastes. However, only two classes of polymeric materials (amorphous fluoropolymers and silicones) have been shown to exhibit appreciable solubility, and this necessitates the use of stabilizing moieties (surfactants) to emulsify CO_2 -insoluble polymers such as polystyrene. SANS and SAXS methods allow the elucidation of the size and shape of both individual molecules and also supramolecular structures [6,7] and this lecture

Figure 2: Aggregation or clustering of deuterium-labelled (PED) in protonated (PEH) polyethylene matrix. The D-labelled molecules form aggregates on slow cooling due to the melting point difference ($\sim 5^\circ\text{C}$) between PEH and PED.

presented some of the first data that have been taken to characterize micellar structures in CO_2 . For example, styrene has been polymerized in CO_2 by means of a polystyrene-b-polyfluoro-octylacrylate (PS-b-PFOA) block copolymer surfactant, which solubilizes the polymer in CO_2 in much the same way as detergents may be used to solubilize oil in water via the formation of microemulsions, as illustrated schematically in figure 4. The experiments to characterize these colloidal aggregates were performed on the ORNL SAXS and SANS facilities [8,9] and the intensities were converted to an absolute ($\pm 4\%$) differential cross-section per unit sample volume [$d\Sigma/d\Omega(Q)$] by comparison with pre-calibrated secondary standards [5,10].

The first small angle scattering study of aggregation mechanisms of copolymer micelles in supercritical CO_2 was undertaken [11] on H_2O -swollen PFOA-g-polyethylene oxide graft copolymers using

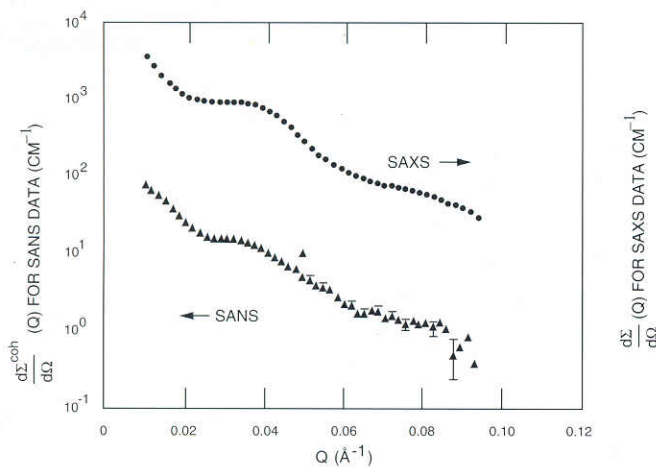


Figure 3: $d\Sigma/d\Omega(Q)$ vs (Q) for deuterated polyethylene sample after subtraction of incoherent background

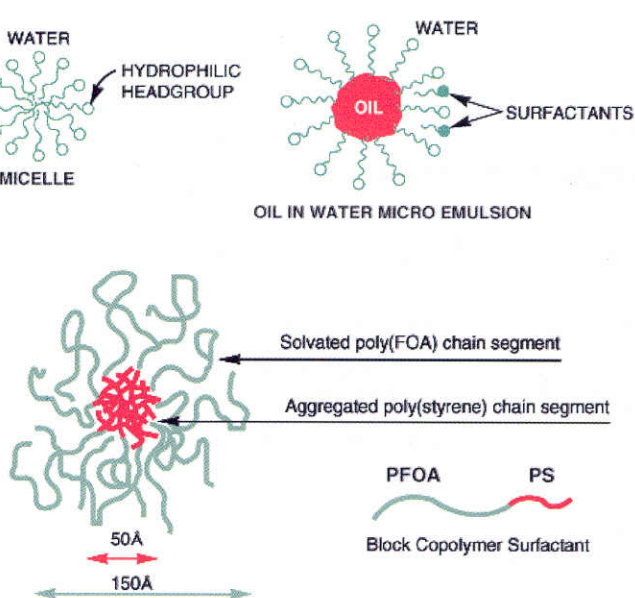


Figure 4: Schematic representation of colloid aggregates in water and supercritical carbon dioxide (above) and model of poly(FOA-b-styrene) micelle in supercritical CO_2 (below).

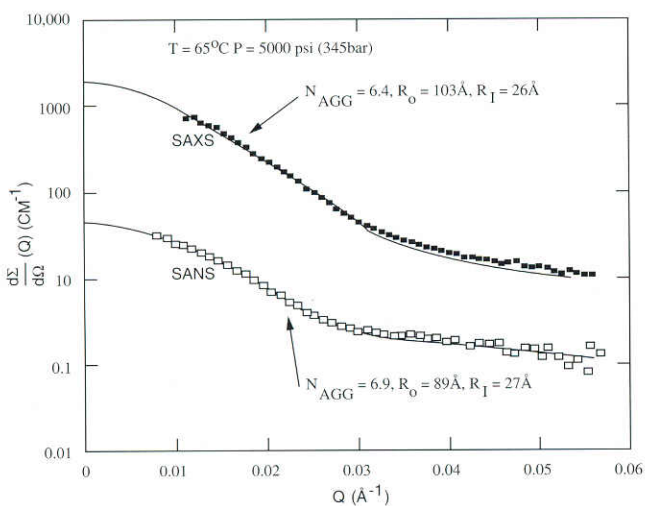


Figure 5: $d\Sigma/d\Omega(Q)$ vs. Q for independently calibrated SAX (solid squares) and SANS (squares) data from 4k/40k PS-PFOA block copolymer micelles in CO_2 .

SAXS, though no calibration of the data was attempted. When this was subsequently accomplished, the initial model parameters were not able to reproduce the measured cross section. Neutron and X-ray scattering are complementary techniques that highlight different components of the structure and we have constructed a high-pressure SAXS cell based on the original design of Fulton and co-workers [11] to facilitate such comparisons. Figure 5 shows a comparison of SAXS and SANS data taken from 4k/40k PS-b-PFOA block copolymer solutions at similar experimental conditions, which were fitted to a spherical core-shell model [7]. The neutron and X-ray cross sections were calibrated independently using secondary standards as explained above. The values of the core radius (R_c) and the aggregation number (i.e. the number of molecules per micelle, N_{agg}) were virtually identical for SAXS and SANS. This forms a useful cross check on the validity of the methodology, as the

contrast factors, and hence the weighting of the components of the structure are quite different for the two techniques.

In order to minimize the time associated with calibration procedures, emphasis is placed on developing pre-calibrated, strongly scattering standards [5,9] which may be run in brief time periods (~1 minute), and figure 6 shows a polyethylene SAXS standard, which has been calibrated with respect to the ORNL suite of SAXS standards [5] for the Daresbury synchrotron SAXS facilities. The peak at $Q \sim 0.0227 \text{ \AA}^{-1}$ is due to the periodic stacking of crystalline lamellae alternating with amorphous regions, with a period $\sim 277 \text{ \AA}$.

References

- [1] A. Guinier and G. Fournet, *Small-Angle Scattering of X-Rays*, Wiley, New York, (1955).
- [2] J. Schelten *et al.*, *Polymer*, **18**, 1111, (1977).
- [3] J. B. Hayter and J. Penfold, *Colloid and Polym. Sci.*, **261** (1983) 1022.
- [4] J. Schelten, D.G.H. Ballard, G. D. Wignall, G. Longman, and W. Schmatz, *Polymer*, **27**, 751, (1976).
- [5] T. P. Russell, J. S. Lin, S. Spooner and G. D. Wignall, *J. Appl. Cryst.*, **21**, 629 (1988).
- [6] D. Chillura-Martino *et al.*, *J. Molecular Structure*, in press.
- [7] J. D. Londono *et al.*, submitted to *J. Appl. Cryst.*
- [8] W. C. Koehler, *Physica (Utrecht)*, **137B** (1986) 320.
- [9] G.D. Wignall, J.S. Lin, and S. Spooner, *J. Appl. Cryst.*, **23**, 241, (1990).
- [10] G. D. Wignall and F. S. Bates, *J. Appl. Cryst.*, **20** (1986) 28.

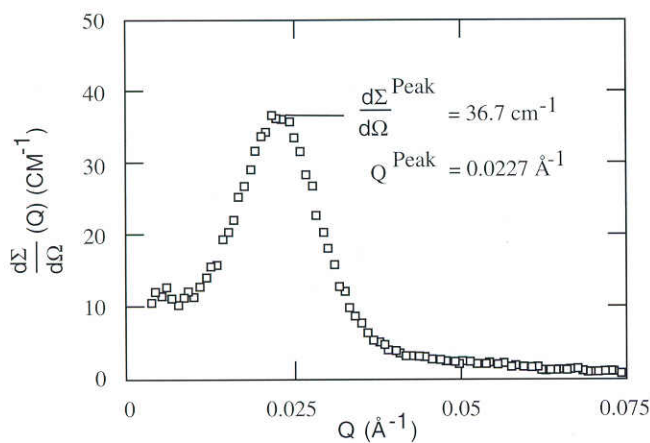
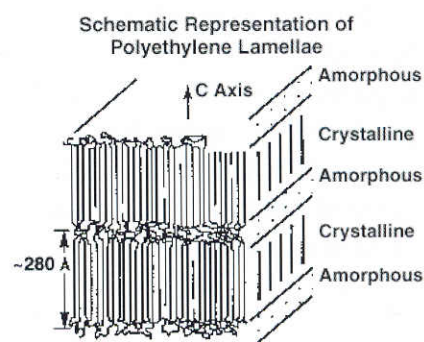


Figure 6: $d\Sigma/d\Omega(Q)$ for S-2907 pre-calibrated SAXS standard



Fibre Diffraction Spot Profiles and the Lorentz Correction

Richard Denny

Biophysics Section, Blackett Laboratory, Imperial College, London SW7 2BZ & CCLRC Daresbury Laboratory, Warrington WA4 4AD.

Introduction

When introducing users to the integration of fibre diffraction intensities using the program LSQINT, the following questions frequently arise:

- i) Does LSQINT apply the Lorentz correction?
- ii) How does it do it?
- iii) What happens at the meridian?

The short answer is that it is all taken care of in the profile calculation but perhaps further explanation would be useful.

The Lorentz correction can be thought of as having two components, the smearing out of Bragg-sampled intensities into annuli due to cylindrical averaging of the intensity transform and the oblique intersection of these annuli with the sphere of reflection. The latter component is dealt with by correct transformation of the image into reciprocal space [1]. However, the first component of the correction still requires attention and that is what is discussed here.

The model fibre

In general, the orientation of a three-dimensional object is specified by three angles, two of which define the orientation of the particle axis and one which defines the orientation of the particle about its own axis. An orientation distribution function (ODF) describes the probability of finding a particle in a given orientation. In an ideal fibre, the particles are assumed to be the same size and cylindrical, with no correlation between the positions of neighbouring particles. The particle axes are distributed about the fibre axis in a cylindrically symmetric manner and for a given orientation of the particle axis, all orientations about the axis occur with uniform frequency, so that the orientation distribution function is dependent on only one angle (figure 1). The particles might exhibit one or three-dimensional crystallinity. Three dimensional crystallinity results in a polycrystalline fibre, giving rise to Bragg-sampled intensity.

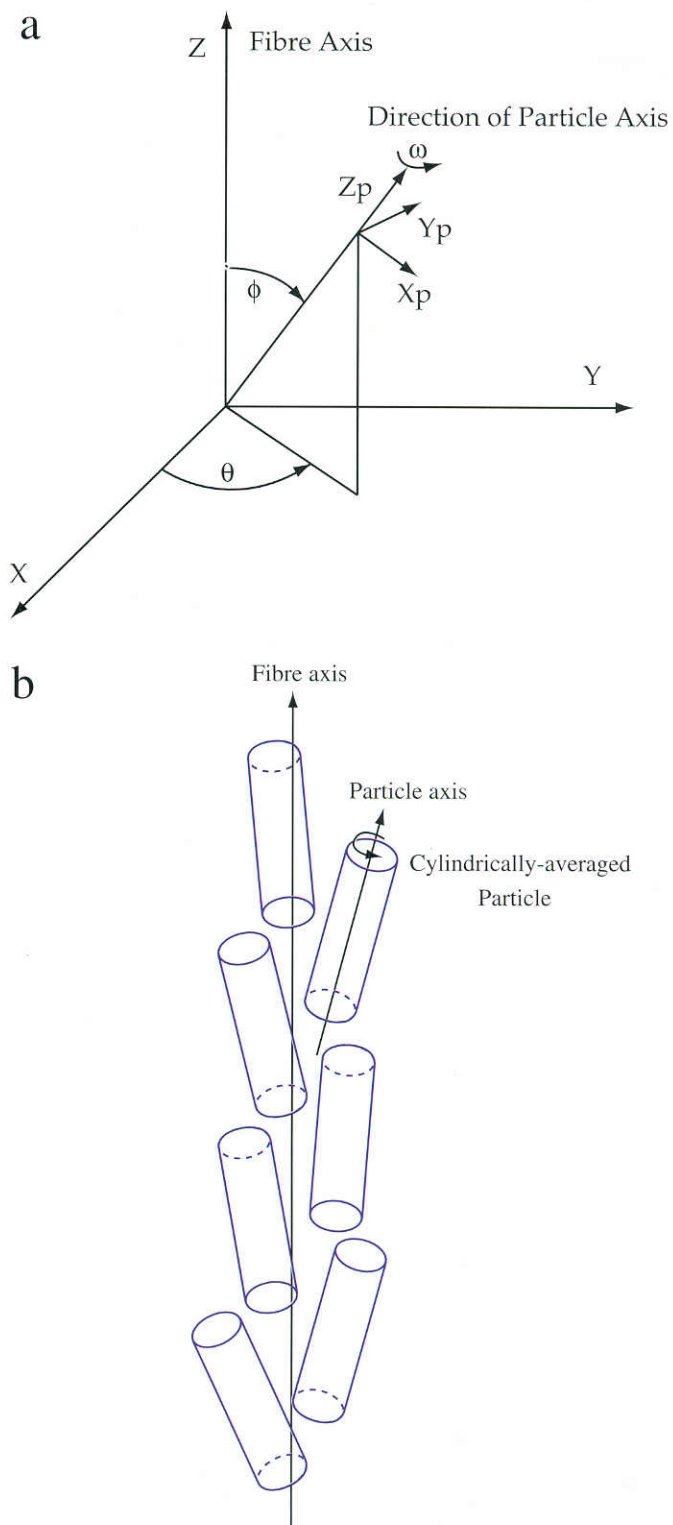


Figure 1: The diagram in (a) shows the angles used to describe the orientation of a particle in three dimensions; the direction of the particle axis is specified by θ and ϕ , while the orientation of the particle and its internal coordinate system about this axis is specified by ω . The diagram in (b) shows a representation of an ideal fibre. All the particles constituting the fibre are cylindrical and of the same size. All values of θ are equally likely, as are all values of ω , so that the orientation distribution function can be written as function of ϕ alone.

Diffraction from a crystalline particle

A diffraction spot from a single particle will have a breadth which is reciprocally related to the particle

size. In general, the Fourier transform of the shape function of the particle $S_{lat}(\mathbf{D})$, is convoluted with the reciprocal lattice $L(\mathbf{D})$, to give the Fourier transform of the finite lattice. This is then squared to give the interference function, *i.e.*

$$Z(\mathbf{D}) = |L(\mathbf{D}) \otimes S_{lat}(\mathbf{D})|^2$$

where \mathbf{D} is a reciprocal space vector. If the $S_{lat}(\mathbf{D})$ on each reciprocal lattice point do not overlap significantly, this can be simplified [2] to

$$Z(\mathbf{D}) = \frac{1}{V_{cell}} [L(\mathbf{D}) \otimes |S_{lat}(\mathbf{D})|^2]$$

For a cylindrical particle, the spot shape can be modelled reasonably well with a Gaussian for the spread in the Z direction and another Gaussian for the radial spread, with widths w_z and w_R , respectively. The particle intensity transform at a point in a cylindrical coordinate system can now be written as,

$$I(R_p, \psi_p, Z_p) = \frac{1}{\pi^{3/2} w_z w_R^2} \sum_{hkl} I_{hkl} e^{-R_p^2/w_R^2 - (Z_p - Z_l)^2/w_z^2}$$

where $R^2 = R_p^2 + R_l^2 - 2R_p R_l \cos(\psi_p - \psi_l)$. The broadening function has been normalized so that, in practice, it is easy to compare integrated intensities from lattices with different degrees of broadening.

This distribution of intensity can be cylindrically averaged, consistent with the requirements of the model that for a given orientation of the particle axis, particles can be found with equal probability at any orientation about that axis,

$$\langle I(R_p, \psi_p, Z_p) \rangle_{\psi_p} = \sum_{hkl} \frac{m_{hkl}}{2\pi \cdot \pi^{3/2} w_R^2 w_z^2} \int_0^{2\pi} I_{hkl} e^{-[R_p^2 + R_l^2 - 2R_p R_l \cos(\psi_p - \psi_l)]/w_R^2 - (Z_p - Z_l)^2/w_z^2} d\psi_p$$

This gives the equation for the cylindrically averaged particle intensity transform (CAPIT),

$$I(R_p, Z_p) = \frac{1}{\pi^{3/2} w_R^2 w_z^2} \sum_{hkl} m_{hkl} I_{hkl} e^{-(R_l - R_p)^2/w_R^2 - (Z_l - Z_p)^2/w_z^2} J_0(2R_p R_l / w_R^2)$$

where $e^x J_0(x) = J_0(x)$, a modified Bessel function.

Here, the summation has been modified to be over the unique intensities and a multiplicity, m_{hkl} associated with each unique reflection has been introduced. This arises as there is systematic overlap of reflections (which are not necessarily symmetry related) due to the cylindrical averaging (figure 2). The cylindrical averaging performed above implicitly provides the velocity component of the Lorentz correction. Figure 3 shows the effect of the averaging on the maxima of diffraction spots of three different widths at varying radii. Curves

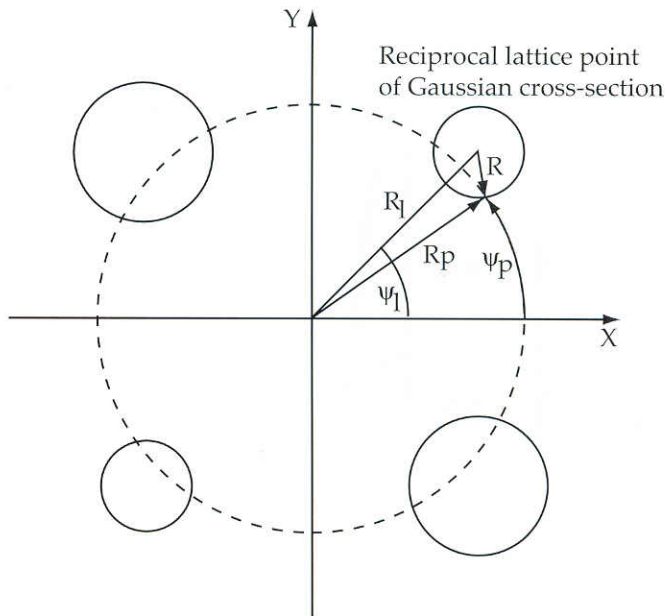


Figure 2: The reflections are assumed to be of Gaussian cross-section (the different sizes of the circles indicates that cylindrical averaging may sum contributions from reflections which are not symmetry related and so are of differing intensity). (R_p, ψ_p) are the coordinates of the lattice point and (R_p, ψ_p) is the point in the particle transform at which the contribution of this lattice point is being considered. The contribution at all points of equal radius must be summed to obtain the cylindrically averaged particle intensity transform.

corresponding to $1/R$ scaled to match the curves calculated from the CAPIT equation, are also shown for comparison. It is clear that the fall-off of intensity depends on the width of the spot. It is also clear that the $1/R$ curve is a better approximation at smaller widths at a given reciprocal radius or larger radii for a given width. The meridian is well-behaved with the averaging approach, the maximum of a spot having the same value it would have if the particle were not cylindrically averaged. This is of course not the case when applying the $1/R$ curve, where the traditional Lorentz correction breaks down completely.

How a point in the particle intensity transform contributes to the specimen intensity transform

So far, only one component of the orientation distribution function has been considered; the cylindrical averaging of each particle about its own axis. In order to calculate the specimen intensity transform, the remaining components of the ODF are convoluted with the intensity distribution from a single particle. As the distribution of particle axes about the fibre axis is cylindrically symmetric, only the dependence on ϕ need be considered. This is achieved by choosing the vector to the desired point in the specimen intensity transform as the axis about

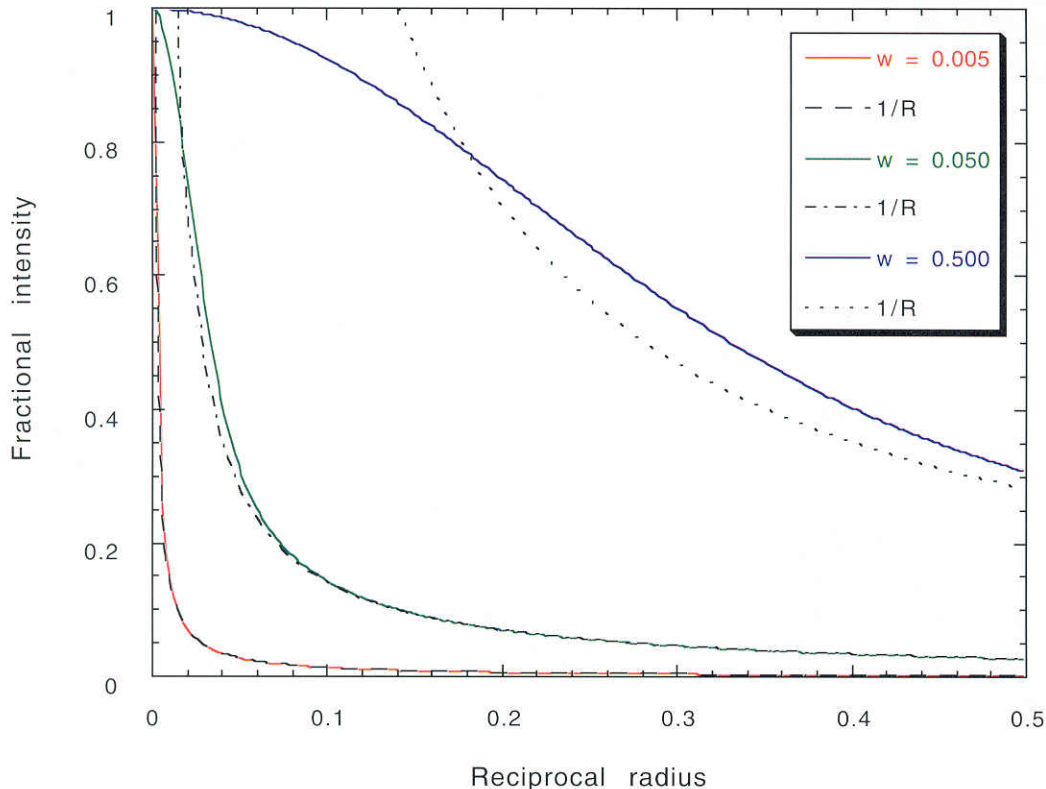


Figure 3: This graph shows the effect of cylindrical averaging reflections. The Y axis is the peak intensity of the averaged reflection as a fraction of its peak value in the three-dimensional particle coordinate system. The red, green and blue curves are the result of applying the CAPIT equation to the situation where $R_p = R_b$, between values of 0.0 and 0.5 on an arbitrary scale for different widths of the Gaussian cross-section of the reflections. The three broken curves show the function $1/R$ scaled to match the curves derived from the CAPIT equation. The coloured curves all intersect the Y axis at 1.0 indicating that meridional reflections have the same peak value in the cylindrically-averaged intensity transform as they have in the three-dimensional

which to integrate (see figure 4). First we consider all those particle axes which will make the same contribution to this point in the specimen transform. These particle axes will form a cone around the axis of integration. We must multiply each point on the base of the cone by the probability of finding a particle axis at that orientation according to the ODF. We can then integrate over all possible cones to complete the convolution [3], *i.e.*,

$$I(D_s, \sigma_s) = \int_0^{\pi} I(D_p, \sigma_p) \sin \sigma_p \int_0^{2\pi} N(\phi) d\xi d\sigma_p$$

where $\cos \phi = \cos \sigma_s \cos \sigma_p + \sin \sigma_s$ and $D_p = D_s$.

The effect of this convolution is to smear the diffraction spots out into arcs. The extent of the arcs modifies the Lorentz correction one would apply to the peak intensity of the diffraction spot. In terms of a traditional Lorentz correction, the fall-off of intensity would go from being proportional to $1/R$ for perfect orientation of the particle axes parallel to the fibre axis to being proportional to $1/D^2$ for powder type disorientation where the particle axes are randomly oriented with respect to the fibre axis. Again, this correction is implicit in the above

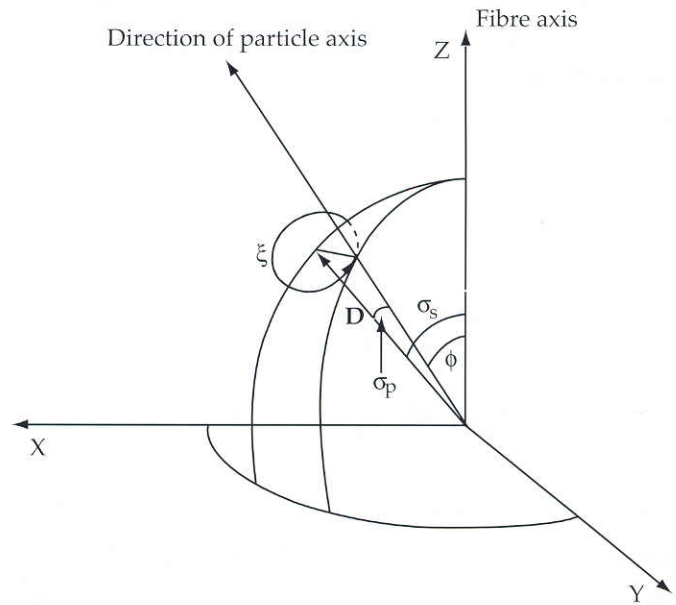


Figure 4: The convolution of the cylindrically-averaged intensity transform with the remaining components of the orientation distribution function (in θ and ϕ) calculated at a point (D, σ) . All particles making the same contribution to this point (*i.e.* all particles whose axes are σ_p away from the vector \mathbf{D}) are summed by integrating over ξ . The integration is then performed over σ_p .

convolution which deals comfortably with the situation where broad diffraction spots lie close to the meridian or the centre of the pattern.

Conclusion

If the traditional form of the Lorentz correction is applied to diffraction spots on a point by point basis, a good approximation to the profile calculation described above is obtained when the spots are not too close to the meridian. However, this method of correcting spot intensities breaks down at the meridian and works poorly where broad spots lie close to the meridian. The method employed by LSQINT naturally applies to these situations and also provides an easy way of scaling together diffraction spots of different widths, possibly from different structures within the same specimen.

References

- [1] Fraser, R.D.B., Macrae, T.P., Miller, A. and Rowlands, R., (1976). *J. Appl. Cryst.* **9**, 81-94.
- [2] Stroud, W.J. and Millane, R.P. (1995). *Acta Cryst. A***51**, 771-790.
- [3] Holmes, K.C. and Barrington Leigh, J. (1974). *Acta Cryst. A***30**, 635-638.

3-D Reconstruction from Fibre X-ray Diffraction Patterns: Myosin-Decorated Actin Filaments

J.J.Harford¹, R.C.Denny¹, E.Morris², R.Mendelson³ and J.M.Squire¹

¹ Biophysics Section, Blackett Laboratory, Imperial College, London;

² Biochemistry Department, Imperial College, London

³ Cardiovascular Research Institute, UCSF, San Francisco.

Helical biological particles such as actin filaments have been studied for many years by electron microscopy and their structures have been determined to about 20Å to 30Å resolution by 3-D reconstruction from single images [1,2]. A big advantage of electron micrographs is that they are real space images of the objects being studied. If one uses methods of reconstruction based on Fourier transforms computed from digitized images, then both amplitude and phase information can be obtained. A single view of a helical object contains many images of the repeating unit on the helix but

with different rotations around the helix axis. Therefore, a single view is sufficient to reconstruct the full helix in 3-dimensions. The main problems with electron microscopy of such biological filaments (often contrasted by using negative staining methods) are that the resolution is usually limited to about 20Å and the amplitude data are uncertain because of the contrast transfer function of the electron microscope.

X-ray fibre diffraction studies from equivalent systems can have the advantage that the diffraction information can extend to about 10Å and beyond and, when properly stripped, the layer-line data should be reliable. However, unlike electron microscopy data, there is little phase information and one cannot directly compute a 3-D reconstruction. This paper discusses the combination, to 27Å resolution, of amplitudes from fibre X-ray diffraction patterns of actin filaments labelled with myosin heads (myosin S1) and phases determined from electron microscopy. It also shows how the structure might be refined to a resolution of at least 13Å, far beyond current electron microscopy data, by modelling using the lower resolution reconstruction shown here as a starting point.

During muscle contraction, force and movement are supposed to be produced by the interaction of the globular heads of myosin molecules with adjacent, helical, actin filaments. The myosin heads are known as ATPases; they bind and can hydrolyse the molecule adenosine triphosphate (ATP) to adenosine diphosphate (ADP) and inorganic phosphate (Pi). This hydrolysis is associated with the release of free energy which is utilised to drive the generation of force and movement. The myosin ATPase is rather slow unless the myosin heads are interacting with actin filaments. In the absence of ATP or ADP, the myosin heads become rigidly attached to actin in the so-called rigor complex. This occurs on death when we stop making ATP and our muscles become 'cross-linked', hence stiff (*rigor mortis* sets in), by the permanent binding of myosin heads to actin.

The myosin molecule is a long (1500Å) coiled-coil α -helical rod on one end of which are two myosin heads. The myosin heads can be separated from the rod by proteolysis, yielding individual, isolated, heads known as myosin subfragment-1 (S1). Such myosin S1 molecules can attach to isolated actin filaments in the absence of ATP to form so-called 'decorated' actin filaments. These have a

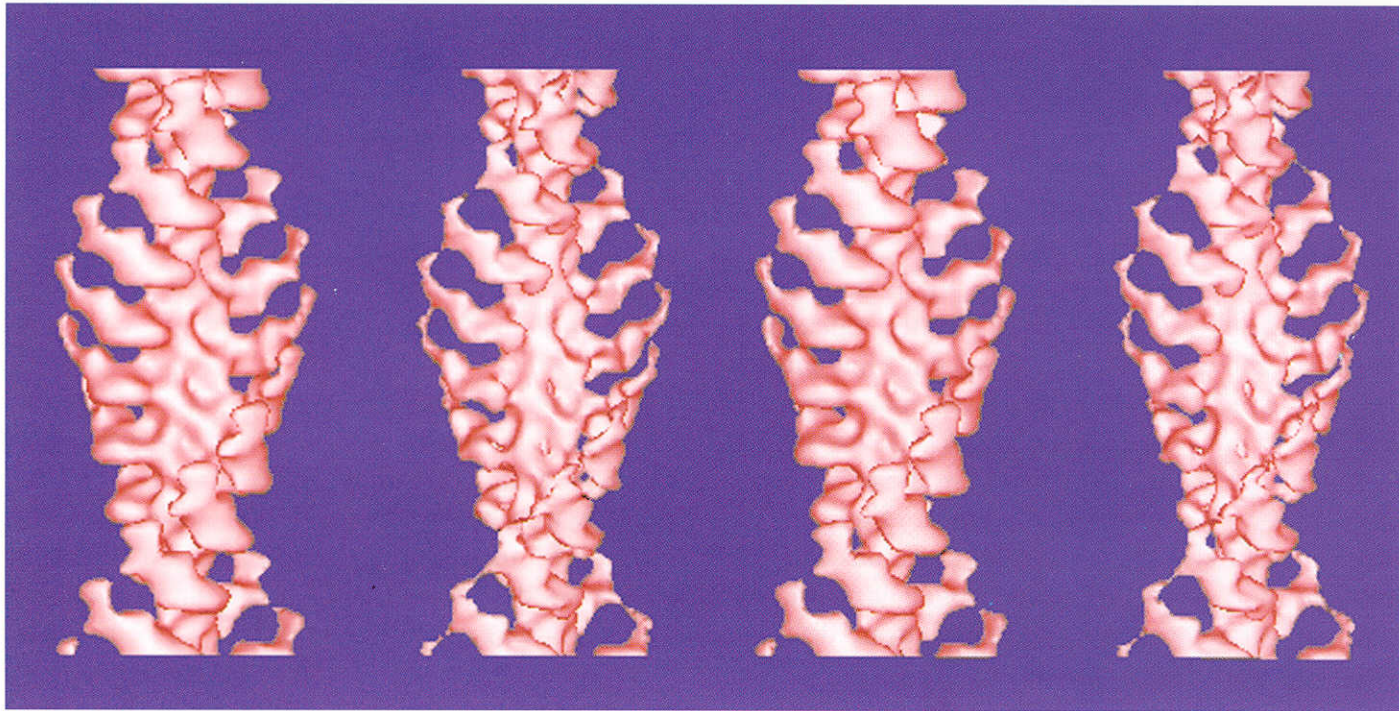


Figure 1: Stereo pairs of 3-dimensional reconstructions of actin filaments ‘decorated’ with myosin heads using (left) electron micrograph data alone [2] and (right) X-ray fibre diffraction amplitudes combined with electron micrograph phases. The axial (cross-over) repeat of the actin filament is about 360 Å.

characteristic pointed appearance; the heads all tilt in the same direction, towards one end of the actin filament. This can be seen in stereo as Figure 1 (left) which is a 3-D reconstruction of decorated actin based solely on electron micrograph data and published by Milligan and his colleagues [2].

Another approach to solving this kind of structure is to soak whole muscle with exogenous myosin S1 in the absence of nucleotide so that the muscle itself then provides an oriented fibre of decorated actin filaments. The X-ray diffraction pattern in Figure 2, recorded on line 16.1 at the CCLRC Daresbury SRS using image plates, shows a very rich layer-line pattern (extending axially to about 27 Å resolution) as stripped using CCP13 programs. The amplitudes from this stripped pattern were then combined with the phases from Milligan’s electron microscopy to give the 3-D reconstruction shown in stereo as Figure 1 (right). This structure therefore has the same resolution as the em reconstruction and it has made use of some em data and some X-ray fibre diffraction data. The work is preliminary so far, but in the end, when fully processed, the X-ray amplitudes should be more reliable than the electron microscopy values. Figure 3 shows that the X-ray reconstruction is quite good because here the known structures of the actin monomer and the myosin head, both determined to atomic resolution by protein crystallography [3,4], have been fitted into the reconstruction. The shapes agree quite well.

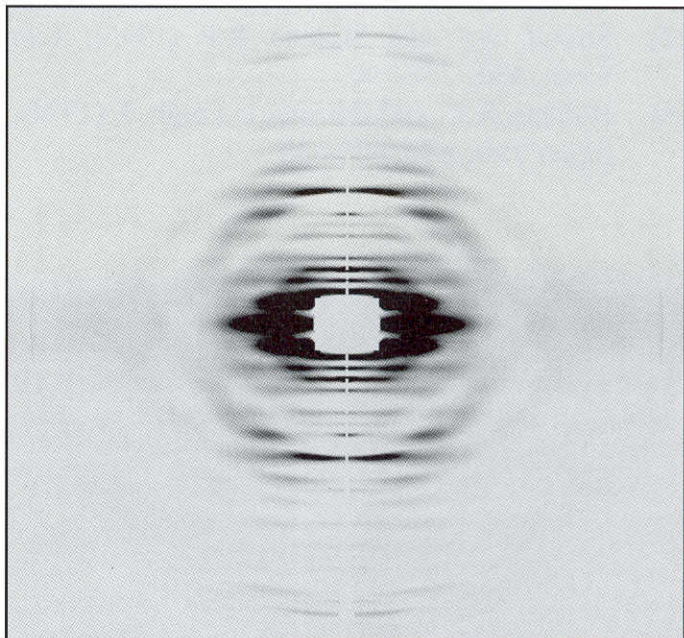


Figure 2: X-ray fibre diffraction pattern (fibre axis vertical) from skinned plaice fin muscle into which a solution of myosin S1 heads has been soaked in the absence of ATP. This effectively produces an oriented fibre of decorated actin filaments as in Figure 1. The myosin head preparation was from chicken pectoralis muscle myosin proteolytically cleaved using the enzyme chymotrypsin. The fibre diffraction data, recorded on image plates on line 16.1 at the CCLRC Daresbury SRS, were stripped using CCP13 software and the displayed image is after background subtraction and layer-line fitting. The outer edge of the pattern corresponds to a resolution of about 25 Å.

So far so good, but layer-lines in the X-ray fibre diffraction pattern shown in Figure 2 actually extend to an axial resolution of at least 13 Å (not shown);

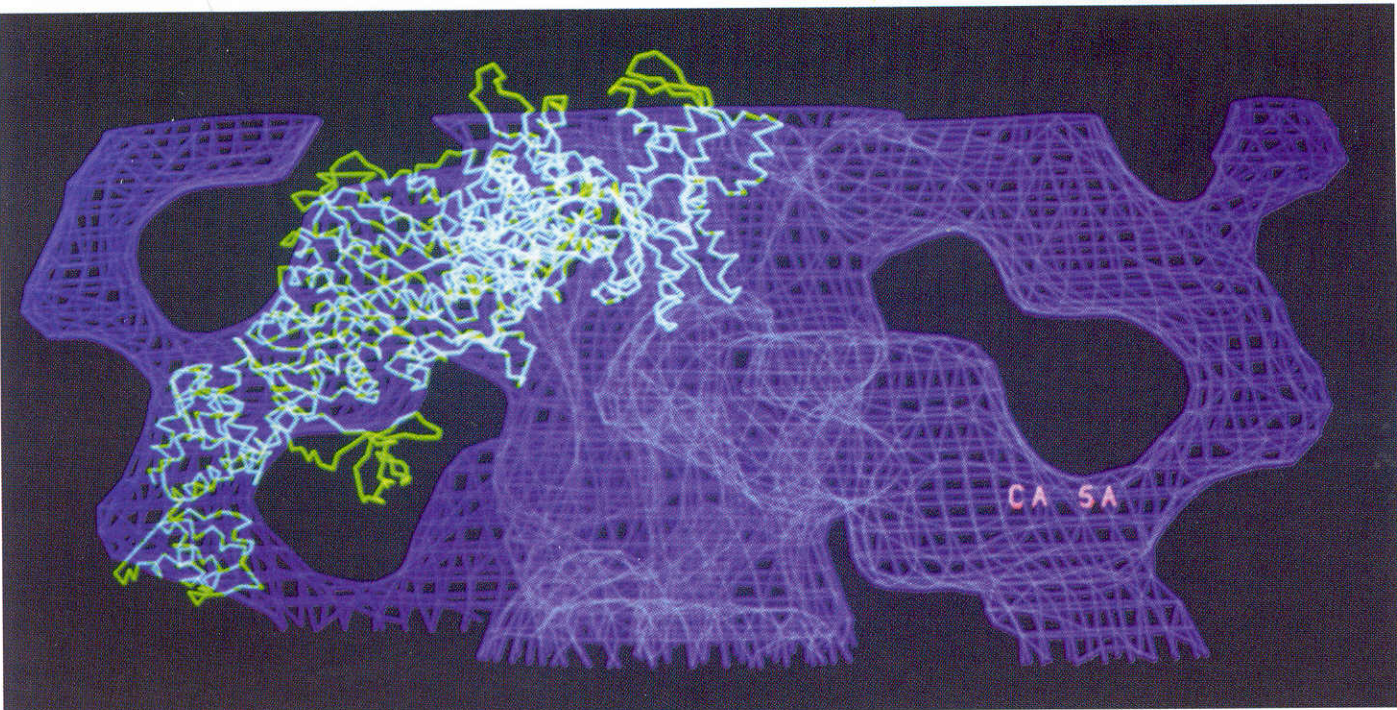


Figure 3: The same 3-D reconstruction as shown in the right hand image in Figure 1, but here represented as a chicken-wire surface using FRODO and into which α -carbon positions in the actin monomer [4] and the myosin head [3] have been fitted. The individual molecular shapes fit the density distribution quite well, but both the reconstruction and the fit have yet to be optimised.

way beyond the current resolution limit (27\AA) of the electron microscopy. How can the decorated actin structure be solved to this higher resolution? In fact, a similar procedure to that used to model the low-angle X-ray diffraction data from myosin filaments in muscle [5,6] can be used once again here. The positioning of the myosin head and actin in Figure 3 provides a good starting point from which to try to refine the structure to be compatible with the X-ray layer-line amplitudes to 13\AA resolution. As in the case of the myosin filaments, the positions of the actin monomer and myosin head can be parameterized, as can more subtle features such as the relative positions of the four sub-domains of the actin monomer and the relative positions of different parts of each myosin head. These parameters can then be refined by a simulated annealing search, together with local minimization, using the structure in Figure 3 as an initial guess. It is evident that the medium resolution combination of electron microscope and X-ray data, followed by high resolution refinement, is a very powerful approach to solving high resolution fibre diffraction data from biological systems.

Acknowledgements

We are indebted to the NCD staff at the Daresbury Laboratory, particularly Liz Towns-Andrews, for their unfailing help, to the BBSRC for grant support,

and to the protein crystallography group at Imperial College for access to their Evans and Sutherland workstation running FRODO.

References

- [1] Moore, P.B., Huxley, H.E. & DeRosier, D.J. (1970) "Three-dimensional reconstruction of F-actin, thin filaments and decorated thin filaments". *J. Mol. Biol.* **50**, 279-295.
- [2] Milligan, R.A., Whittaker, M. & Safer, D. (1990) "Molecular structure of F-actin and location of surface binding sites". *Nature* **348**, 217-221
- [3] Rayment, I., Rypiewski, W., Schmidt-Base, K., Smith, R., Tomchick, D., Benning, M., Winkelmann, D., Wessenberg, G. & Holden, H. "Three-dimensional structure of myosin subfragment-1: a molecular motor". (1993) *Science* **261**, 50-58.
- [4] Kabsch, W, Mannherz, H.G., Suck, D., Pai, E.F. & Holmes, K.C. (1990) "Atomic structure of actin: DNase I complex". *Nature* **347**, 37-44.
- [5] Hudson, L., Harford, J.J., Denny, R. & Squire, J.M. (1995) "An actin's eye view of myosin: SAXS meets PX". *CCP13 Newsletter*, **4**, 20-23.
- [6] Hudson, L. (1996) "Ultrastructure of the A-band unit cell in relaxed muscle". Ph.D Thesis, University of London.